Appendix G – Technology Trends and Risk Considerations

Dewberry acknowledges the assistance of Dr. Chris Parrish and David Doyle of the National Geodetic Survey, and Lorraine Tighe of Intermap Technologies, Inc. in providing technical input and editing of Appendix G.

Topographic LiDAR System Technologies

Evaluate trends in sensor and positioning technology and the potential impact(s) of these trends on: 1) the ability to satisfy Business Uses, 2) the costs of implementing a national program over a 4-7 year timeframe, and 3) developments that might affect the timing and duration of the program.

Airborne LiDAR remote sensing technology has advanced very rapidly in the past 2 decades. In the late 1980s and early 1990s advances in LiDAR sensor technology were mainly initiated by federal agencies such as NASA; however, since the mid-1990s the commercial industry has made significant contributions in the research and development of high-accuracy, high-pulse-rate (including multiple-pulses-in-air – MPiA) LiDAR systems and more accurate and efficient scanning mechanisms to enable high-altitude (up to 3000 m), wide-area topographic mapping. From a national mapping perspective, these enhancements have enabled the mapping of several state-wide data acquisitions. Most of these data collects have been focused on determining bare-earth terrain in support of FEMA and USGS programs and state and local agencies. From a National Enhanced Elevation Assessment perspective, these data sets do not always provide the necessary consistent information at the appropriate Quality Level for other derivative products such as vegetation, biomass, fire-fuel estimation, land cover, geologic, and coastal mapping.

Lasers

With the advent of new and improved laser technologies, applications of LiDAR in terrain mapping are rapidly growing. The new lasers being developed emit highly-collimated pulses that have (1) shorter pulse width, thereby enabling increased measurement accuracy and enhanced multiple-return pulse resolution, (2) higher pulse power for operating at higher altitudes, (3) reduced beam divergence and receiver field-of-view to improve spatial accuracy of the laser footprint, and (4) higher pulse rates (200-500 KHz) to allow for greater sampling density at higher operating altitudes. However, tradeoffs exist between the laser-characteristics described above; for example, higher pulse power limits the laser's ability to generate pulses at a higher rate. While laser technology has improved, there has been significant research and development in the other parameters that affect laser ranging, including the sensitivity and response time of the detector, the system signal-to-noise performance, the detection threshold, implementation of the ranging electronics, full-waveform digitization, and vast enhancements in processing and analysis software. Typically, a high-energy pulse required for laser ranging has a relatively broad pulse width. Recent advances in laser diode technology, including gain switching – a technique for generating short optical pulses in a laser by modulating the laser gain, and use of fiber lasers as compared to solid-state lasers, have enabled pulse widths of 800 picoseconds at acceptable pulse peak power for airborne laser ranging.

As such, the trend in the commercial LiDAR industry has been to offer higher sampling rate to increase data density and/or operate at higher altitudes for more efficient coverage. The federal sector has

primarily focused on developing LiDAR systems for very high-altitude / spaceborne missions. Although there is some overlap, the research and development between the public and private sector has been complimentary, leading to more accurate and efficient LiDAR sensors for wide-area mapping.

Full-waveform digitization

Another trend in LiDAR sensor technology is the full waveform digitization of the return pulse. Traditional discrete-return LiDAR systems typically record several (up to five) returns for each laser pulse. Full waveform digitization of a laser pulse creates a pulse-by-pulse reflection record that is highly sensitive to even minor changes in vertical structure. This technique enables many multiple returns with short separation to be collected from a single laser shot. This is especially true for a short-temporal-pulse-width laser pulse. The ability to detect separate returns from closely spaced surfaces is relevant for detection of ground returns beneath short-stature vegetation. Further, deriving forest measurements related to volume and canopy structure can benefit from the fine resolution between successive returns from the vegetated canopy. In contrast, discrete-return LiDAR systems require a minimum object separation to register consecutive returns from the pulse separately, thereby being blind to canopy material within this "dead zone" (Figure G.1).

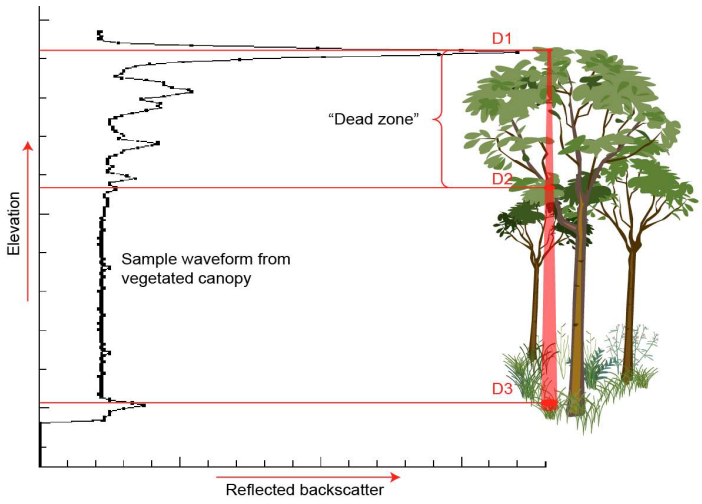

Figure G.1. Schematic showing the dead-zone effect in discrete return LiDAR systems. 'D1', 'D2', and 'D3' are successive reflections from a discrete return laser pulse. The laser pulse is effectively blind to canopy material between 'D1' and 'D2'. The vertical structure information is, however, captured in the sample waveform from a vegetated canopy acquired by a small-footprint waveform-resolving system. [Source: Nayegandhi & Brock, 2008]

The dead zone, which typically ranges from 1 m to greater than 7 m in vertical height, is usually caused by the duration of the pulse (i.e. pulse width) and the hardware limitations in sensor design. In waveform systems, small variations in the vertical structure can be detected by processing the resulting waveforms using a variety of pulse detection methods. A number of detection methods can be applied on the backscatter waveform in post-flight processing software: threshold, center of gravity, maximum, zero crossing of the second derivative, and constant fraction. Determining the range in post-flight processing software has the advantage of selecting one or more pulse detection algorithms based on the application, analyzing the intermediate results, and considering neighborhood relations of pulses. Many commercial systems now provide the option to digitize the return waveform in 1-nanosecond increments. However, third-party software to process waveforms is lacking and there are no standard formats and guidelines for storing waveform data.

Photon counting

Discrete-return and waveform-resolving LiDAR sensors described above are examples of analog ranging, wherein a detector converts received optical power into an output voltage for the entire laser pulse,

yielding signal strength as a function of time. These analog systems require high signal-to-noise (SNR) performance per pulse to accurately determine the range to the illuminated target. Another technique, known as single-photon counting, can be used to record the arrival of single photons from the transmitted laser pulse. Combining a photon counting detector with timing electronics, the time-of-flight between the transmitted laser and reception of a single photon is recorded (Figure G.2).

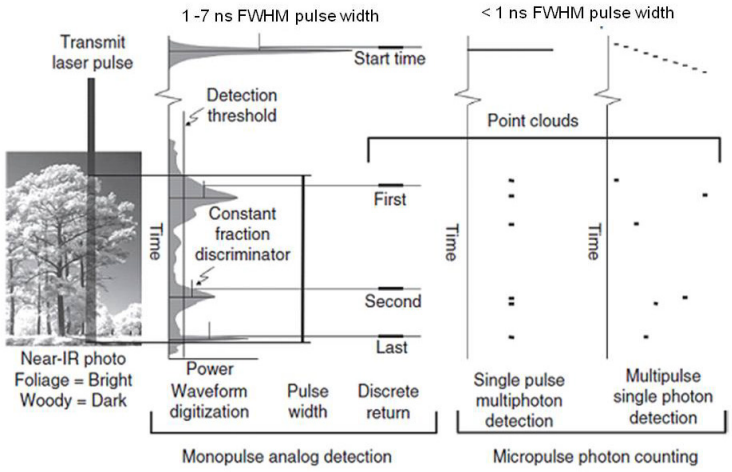

Figure G.2. Illustration of laser ranging methods, depicting transmit pulses and received signals from a multi-storied forest canopy as recorded by analog detection and photon counting approaches [Adapted from Harding, 2009].

Accumulation of many single-photon ranges can recreate the height structure of the target. In order to minimize the effect of solar background noise, the detection of energy at all wavelengths other than that of the laser is blocked. A small receiver field-of-view is also used to restrict the collection of light to the location illuminated by the laser. However, solar photons are a very significant noise source for a photon counting detector, and hence most photon counting LiDAR missions are limited to nighttime operations.

Another limiting factor for single-photon counting LiDAR systems is the inability to compensate for the brightness of the target. A large number of photons will be directed back to the sensor from a bright target as compared to a dark target at the same height. This often results in the bright target appearing higher than the dark target (an issue sometimes referred to as "Range Walk"). In this case, the transmitted LiDAR pulse is not being detected by an analog detector that records the entire pulse and has the ability to correct for range walk using a constant-fraction (or other) method. As a result, the photon-counting detector cannot directly correct for range walk by detecting single photons. Several research initiatives are looking to address these specific limitations described above.

Photon counting systems have 2 distinct advantages over traditional analog-detection LiDAR systems: (1) they require much lesser power, thereby enabling sensing from small unmanned aerial vehicles or satellites, and (2) the significant reduction in laser power can allow for very short-duration pulses (< 100 picoseconds) which can significantly increase the fidelity of terrain reconstruction. Research systems such as the Slope Imaging Multi-polarization Photon-count LiDAR (SIMPL) are being developed by NASA to demonstrate measurement approaches of benefit for improved, more efficient spaceflight laser altimeter missions.

Flash LiDAR

Flash LiDAR systems are analogous to a camera with a flashbulb, but with the flash being provided by laser illumination and the use of a detector with a high-precision clock to determine the time it takes for the flash to depart, reflect off the target, and return. By measuring the time of flight of the reflected

laser pulse, the sensor can determine a range measurement along with intensity for each pixel in the image. The entire scene within the sensor's field of view (FOV) is imaged with a single flash of a laser (i.e. a single laser pulse). The resulting product over the range of all detector pixels is a 3D LiDAR image. Each pixel within the image is correlated in time, which makes the sensor insensitive to relative motion between the aircraft/spacecraft and the target, thereby eliminating the need for complex processing algorithms to account for relative motion of the laser scan over the FOV. Similar to photon-counting LiDAR systems, Flash LiDARs use a short-duration, low-power, light-weight laser. The elimination of the scanner in Flash LiDAR ensures a solid-state system with no moving parts and also reduces the overall weight of the system considerably; making it a natural fit for long range spacecraft missions as well as short range unmanned autonomous vehicles.

In February 2011, the DragonEye 3D Flash LiDAR camera, developed by Advanced Scientific Concepts, Inc., was launched on the final spaceflight of Discovery. Capable of capturing a full array of 128x128 independently triggered 3D range pixels per frame up to 30 frames per second in real-time, the DragonEye is designed to be used for Automated Rendezvous and Docking and possible On-orbit Satellite Servicing. The system was tested as part of the scientific payload on Discovery.

Flash LiDAR has the potential to find its way into 3D surveying applications as well. However, some of the limitations of the current technology are similar to those encountered by Photon-counting LiDAR sensors (i.e. range walk and solar noise). Additionally, the resolution of current commercially available Flash LiDAR cameras is 128x128 pixels. This low resolution requires the use of a very small field of view. Given the similarities to technology in digital photography, the resolution is likely to advance to the megapixel range within the next decade, and the cost should reduce significantly with the economy of scale.

Enabling Technologies (applies to both LiDAR and IFSAR)

Precise positioning and orientation data provided by Differential Global Positioning System (DGPS) and GPS-aided Inertial Navigation System (INS) have been instrumental in creating accurate topography datasets. It was the development of these enabling technologies that led to the commercialization of airborne LiDAR and IFSAR in the mid-1990s. "Direct georeferencing" (DG) is the direct measurement of the position and orientation parameters of a remote sensor that is required to stabilize and register the acquired data in geographic coordinates. Currently, almost all commercial airborne LiDAR surveys require the use of one or more GPS base receivers (also known as reference receiver) at known positions to differentially correct the GPS data acquired by the onboard receiver. Current standard operating procedures typically require the baseline separation between the roving and reference receiver to be limited to 25-30 km for LiDAR surveys and 50-300 km for IFSAR surveys. GPS base receivers are generally deployed on known benchmarks or occupied for a 24-hour period on a temporary benchmark to accurately locate the position of the receiver using the Online Positioning User Service (OPUS) solution provided by NOAA's National Geodetic Survey (NGS). From a national mapping perspective, this poses a significant challenge and considerable cost to deploy base receivers every 25-30 km within the LiDAR survey area. On the other hand, IFSAR surveys require less deployment of base receivers. In many circumstances, it is impossible to access certain remote areas to deploy a base receiver. Further, base receivers require an unobstructed view of the horizon, which is difficult to find in vegetated and

mountainous terrain. DG is often the most significant contributor to the overall "error budget" of the resulting data, and requires significant mission planning to avoid or diminish its limitations.

GPS Modernization

Several technological advances in the past few years and into the next decade are likely to alleviate the "short baseline separation" problem and improve the overall quality of GPS data. GPS is part of a growing set of Global Navigation Satellite System (GNSS), which include the (existing) Russian GLONASS, upcoming European Union's Galileo and Chinese COMPASS systems. Enhanced satellite coverage offered by these systems can be used by GPS receivers for improved positioning reliability and faster ambiguity resolution. Upgrades to the receiver electronics and firmware have reduced the latency in the time to triangulate the real-time position of the sensor. GNSS receivers, such as NovAtel's next generation OEM6 product platform provides high performance scalable positioning options and low latency positioning with high data rates that can be used to access all current and upcoming GNSS satellite signals.

The Office of Space Commercialization has initiated a GPS modernization program to upgrade the GPS with new, advanced capabilities to meet growing military, civil, and commercial needs. The central focus of the GPS modernization program is the addition of new navigation signals to the GPS constellation. Three new signals will be added for civilian use: L2C, L5, and L1C. L2C enables faster acquisition, enhanced reliability, and greater operating range. The stronger L2C signal and forward error correction will improve GPS mobile, indoor, and other uses. When combined with L1 C/A in a dual-frequency receiver, the user can calibrate and remove the effects of the ionospheric delay error for that satellite in a position solution. L5 is the third civilian GPS signal, modulated onto 1176.45 MHz and transmitted with considerable higher power (3 db more) than the L1 signal. L5 is broadcast in the radio band reserved exclusively for aviation safety services making it easier to manage interference in this band than is possible in L1 and L2 bands. When used in combination with L1 C/A and L2C, L5 will provide a highly robust service that may enable sub-meter accuracy without augmentations, and very long range operations with augmentations. L1C is the fourth civilian GPS signal, designed to enable interoperability among GNSS. L1C is designed to improve mobile reception in cities and other challenging environments. Currently, there are 8 satellites in the GPS constellation that broadcast L2C, and one satellite normally broadcasting L5. The broadcast of the first L1C signal with GPS III is currently scheduled for 2016.

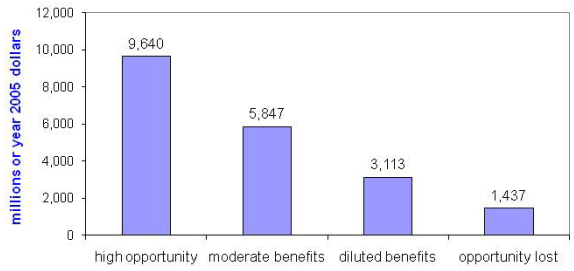

Figure G.3. Net Benefits of all L2C Users based on certain scenarios [Source: Leveson, 2006].

A cost/benefit analysis study conducted in 2006 focused on the L2C applications other than those of aviation and military uses. The study concluded that L2C will substantially benefit dual-frequency applications until alternative signals are widely used and could be a long-term boon for applications requiring three or more frequencies. The net benefits ranged from $1.6B to $9.6B through 2030, depending on several scenarios outlined in the study (Figure G.3). For the most likely scenario, the net benefit was $5.8B, which was about 20x the equipage costs.

CORS Network

The National Geodetic Survey (NGS), an office of NOAA's National Ocean Service, manages a network of Continuously Operating Reference Stations (CORS) that provide GNSS data consisting of carrier phase and code range measurements in support of three dimensional positioning, meteorology, space weather, and geophysical applications throughout the United States, its territories, and a few foreign countries. The CORS network is a multi-purpose cooperative endeavor involving government, academic, and private organizations. The sites are independently owned and operated. Each agency shares their data with NGS, and NGS in turn analyzes and distributes the data at no cost to the user. As of June 2011, the CORS network contains over 1,800 stations, contributed by over 200 different organizations, and the network continues to expand (Figure G.4).

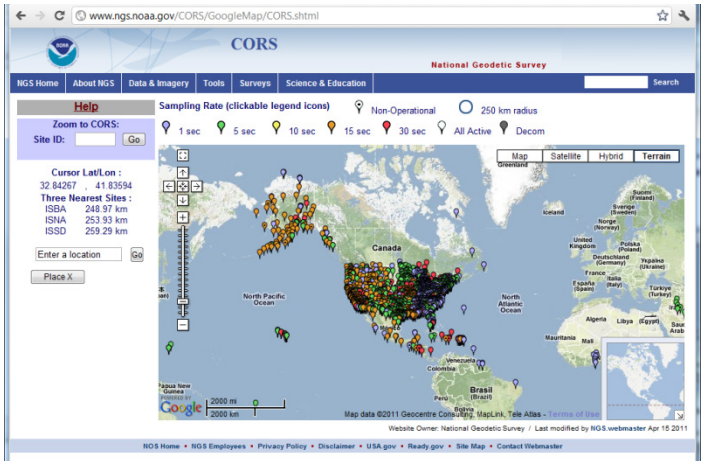

Figure G.4. NOAA NGS CORS network as of June 2011 includes over 1,800 stations, many of which operate at 1 second interval.

According to the NGS Ten-Year Plan published in 2008, the CORS network will be transformed into a two-level system whose first (very small) level is made of NGS-owned or –operated "foundation" sites treated as critical infrastructure. These foundations sites will ensure that the National Spatial Reference System (NSRS – to be based on the new geometric "horizontal" datum that replaces NAD83 by 2018) is accurately tied to the International Terrestrial Reference Frame (ITRF) and accessible to GNSS users in a minimally acceptable fashion anywhere in the United States and its territories. The second (very large) level of the CORS network includes all the other sites, which are positioned relative to the foundation and whose maintenance and quality control fall to the site operators. This transfer of responsibility will enable NGS to concentrate on day-to-day maintenance of the foundation CORS, thereby fulfilling its mission of defining, maintaining and providing access to the NSRS. Tools such as OPUS-GNSS, capable of computing coordinates for any number of stations with any combination of constellations, signals and data collection times will be developed and provided. An OPUS-GNSS solution is dependent on the predicted satellite ephemerides and clock corrections that are broadcast in the navigation message in real-time. A precise ephemeris solution is usually provided by the International GNSS Service (IGS) within one week. In essence, the NGS vision is that by 2018, the three dimensional coordinates of the orbits of any satellites monitored by the CORS network should have an accuracy of about 1 centimeter at any time, and less than a centimeter with a precise ephemeris solution.

As part of the National Geodetic Survey's (NGS) continuing efforts to improve the NSRS, NGS announced the National Adjustment of 2011 (NA2011) project in May 2011. The NA2011 Project will yield updated North American Datum of 1983 (NAD 83) coordinates on approximately 80,000 NGS passive control marks positioned using GNSS technology. The new adjustment will ensure passive GNSS marks are optimally aligned with the CORS network.

Real-time Networks and Precise Point Positioning (PPP)

The need for GPS reference stations may be completely eliminated if direct georeferencing can be achieved using real-time network technology or other post-processing methods such as precise point positioning (PPP). Real-time applications, such as the GPS Real-time Kinematic (RTK) solutions have seen enormous growth in the past decade. A variety of RTK applications exist today, ranging from a single base/rover pair used by a single surveyor, to city and state governments installing networks of base stations and providing a service to rover users. NGS, as part of its ten-year plan, will support RTK applications by certifying the RTK network operators as "NSRS compliant", thereby ensuring compatibility with each other and with NSRS in general. NGS also plans to provide CORS data over the Internet to enable real-time CORS data streams. Currently, the CORS data are available for download about an hour after it is collected. NGS estimates that the instantaneous data streams will promote the development of real-time positioning applications at around 1-meter level. For airborne LiDAR operations, this medium-accuracy will not be sufficient for deriving accurate digital elevation models at the centimeter level. However, it is hoped that the real-time CORS data streams will enable greater expansion of local RTK networks that provide centimeter-level accuracy. A secondary benefit of real-time CORS data streams is the possibility to improve OPUS-GNSS such that the amount of data required for a solution will be reduced to a few minutes, possibly a few seconds, and sharing these results instantly via an online NGS database. This secondary benefit could potentially enable near real-time direct georeferencing of LiDAR data if data systems onboard the aircraft are able to access the NGS database and have the processing power to integrate the GPS, INS, and laser ranging data.

Precise point positioning (PPP) has recently been suggested to be a viable alternative to differential methods for precise positioning using GNSS. PPP does not require any local or regional reference stations and can provide sub-decimeter accuracy for kinematic applications. PPP involves the use of only one receiver (compared to the need for a base and roving receiver when using differential methods). High accuracy is achieved by replacing the broadcast navigation message with precise post processed values from e.g. the International GNSS Services (IGS). It is not possible to resolve carrier phase ambiguities using single-receiver observations. However, the carrier phase ambiguities can be estimated using a float solution with a span of continuous observations. Typically, the accuracy of the PPP solution improves considerably with time of continuous operation; for example, a kinematic solution with 24 hour operation has an estimated RMS horizontal and vertical accuracy of 0.03 m and 0.04 m respectively, whereas the same solution with only 1 hour of operation has an estimated accuracy of 0.15 m and 0.20 m respectively (using Frontier Geomatics TerraPOS software). Tropospheric and ionospheric delays in the signal for single receiver observations need to be adjusted using *a priori* information and empirical models that are available from IGS. Factors that contribute to the geometrical strength of using PPP include the number and distribution of available satellites, elevation cut-off angle, length of time span with continuous carrier phase observations, and dynamics of the satellite receiver. Aside from the significant savings in cost and time related to deploying reference receivers, the PPP is a homogenous solution unlike a DGPS solution which heavily depends on the distance to the base station. Results from use of PPP solutions for airborne LiDAR and IFSAR surveys have not been extensively documented but internal reports and white papers from various LiDAR and IFSAR acquisition vendors suggest that the PPP solution offered by the TerraPOS software (LiDAR

surveys) and proprietary software (STARNAV, Intermap's IFSAR) are viable alternatives to DGPS solution for achieving GPS positioning accuracies of 5-30 cm.

In general, most commercial LiDAR vendors prefer to use traditional differential methods with short baseline separation for LiDAR surveys that require Quality Level 3 or better accuracy. One of the biggest concerns is the lack of confidence in using long baselines or PPP solutions during survey operations. It is cost-prohibitive to redeploy an aircraft and LiDAR sensor if positioning and orientation information are not accurately acquired. Hence, most commercial vendors use the PPP solution as a backup alternative in case of errors in the DGPS solution due to the data acquired by the reference stations.

Geopotential ("vertical") Datum – GRAV-D – The New "Geoid" model

Gravity for the Redefinition of the American Vertical Datum (GRAV-D) is a proposal by NGS to re-define the vertical datum of the United States by 2021. The accuracy of the proposed gravity-based vertical datum is expected to be 2 cm for much of the country. The current North American Vertical Datum of 1988 (NAVD88) based on the Geoid model, exists only for the conterminous North American continent, and relies on passive benchmarks that are not regularly maintained and don't exist in many places (especially in Alaska). Further, NAVD88 suffers from a zero height surface that has been proven to be ~50 cm biased and ~ 1 m tilted across CONUS based on the most recent independently computed Geoid model from the GRACE satellite (Figure G.5).

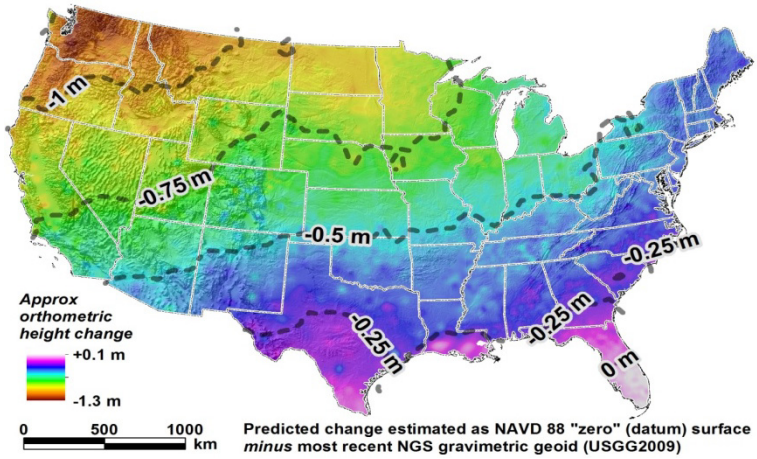

Figure G.5. Approximate predicted change from NAVD88 to the new vertical datum. [Source: Smith & Roman, 2010.

The GRAV-D project consists of three major initiatives: (1) A high-resolution "snapshot" of the gravity in the US to be achieved by airborne gravimetric surveys at an estimated cost of ~$39 million. The highest priority targets are Alaska, Puerto Rico and the Virgin Islands, the Gulf Coast, the Great Lakes, and Hawaii. The airborne gravity mission is expected to survey the entire US and its holdings by 2022 (given appropriate funding). (2) A low-resolution "movie" of gravity changes determined by a terrestrial campaign of monitoring geographically dependent changes to gravity over time at specific absolute gravity sites nearby or at each airport of operations. (3) Regional partnership surveys with local (governmental, commercial, and academic) partners who can support airborne or terrestrial surveys or monitor local variations in the gravity field. Thus, the GRAV-D project seeks to establish a new vertical datum by 2022 that is based on the true Geoid as determined by the local time dependent nature of the gravity field and also accounts for the rise of global mean sea level. Until 2022, hybrid Geoid models that are continuously being updated by the NGS Height Modernization program will be used as the official vertical datum.

Inertial Navigation Systems

GPS-Aided Inertial Navigation Systems (GPS-AINS) now offer a turnkey approach to direct georeferencing. The Inertial Measurement Unit (IMU) containing the accelerometers and gyros has reduced in size significantly, allowing it to be located at or close to the desired instrumentation point (typically, the sensor reference point is defined as the "origination" point of the laser beam, e.g., the center of the scan mirror) and are becoming more readily available. Traditionally, high quality inertial systems were required to be very large in size for obtaining required level of orientation accuracy. New algorithms have recently been developed to remove the short term noise in the low cost inertial sensors, thereby making them applicable for direct georeferencing. Post-processing software for GPS and IMU data uses the Kalman filter's inertial navigation errors to correct the position, velocity, and attitude computations in the inertial navigation algorithm. This error correction closes the loop around the INS and thereby regulates the INS errors to be consistent with the aiding sensor errors. In a GPS-AINS, it regulates the INS position and velocity errors to be consistent with the smoothed GPS position and velocity errors. Thus a GPS-AINS is able to align from a cold initialization while the aircraft is in motion, and can produce accuracy better than a free-inertial attitude system, thereby allowing the use of lower quality inertial sensors. The GPS-AINS post-processing software thus plays a very important role in the overall accuracy of the INS, and considerable research is invested in improving methods to reduce the INS errors in post-flight processing. The Applanix POS-AV solution and NovaTel's Inertial Explorer are the primary software suites used to process GPS-AINS data. The PPP solution, offered by TerrPOS and explained above, can also be ingested into these software if no base stations are used during data acquisition.

Topographic LiDAR Outlook

As explained in the sections above, several exciting developments in laser ranging, GPS/GNSS, and IMU technology are expected in the next decade. Recent improvements in laser diodes, detectors, and ranging electronics have enabled the acquisition of accurate and high density data. A suite of survey platforms are now offered by several LiDAR manufacturers such that the systems are catered towards specific applications. Among these platforms, the long-range systems use a powerful laser source, high pulse repetition frequency, multiple-pulses-in-air (MPiA) technology, and large scan angles to create a very wide swath at high operating altitudes. From a national mapping perspective, these developments enable efficient mapping of large regions at Quality Levels 1, 2 and 3. For specific applications such as corridor mapping that require very high-density data with high-precision results, light-weight, ultra-compact LiDAR systems are available for deployment on small aircraft and helicopters. Further, the digitization of the return pulse (waveforms) and the smaller laser pulse widths have enabled improved vertical resolution (i.e., more information about vertical structure). Although waveforms can considerably increase the size of the data set and present a big challenge for data processing and storage / access, the benefits of added and improved derivative products from waveform may outweigh the cost associated with the increased data volume, depending on the application. A detailed study on the cost/benefit analysis for waveform would need to be conducted for a more detailed analysis. For very high altitude surveys or a spaceborne deployment, single-photon-counting and Flash LiDAR systems

appear to be the most viable solution due to their low laser power requirement in a narrow, eye-safe beam. However, the research on single-photon counting and Flash LiDAR systems is still in the early stages, and several current operational constraints need to be resolved in order to commercialize this technology and apply it to a national mapping perspective.

Topographic LiDAR Technology Conclusions

- Technology trends show continued evolutionary improvements in topographic LiDAR system technologies, but not revolutionary improvements that would justify delays in implementing a national elevation program over a 4-7 year timeframe.
- All Business Uses with mission-critical requirements for LiDAR data can be satisfied with today's topographic LiDAR technologies so that the major benefits could be realized without delaying program implementation.
- Evolving topographic LiDAR technologies will improve LiDAR acquisitions in the next decade but the expectation of improved capabilities should not delay implementation of new enhanced elevation programs.

Topographic LiDAR Figure References

Figure G.1: Nayegandhi, A., Brock, J.C., 2008, Assessment of Coastal Vegetation Habitats using LiDAR. In: Yang X.(ed) "Lecture Notes in Geoinformation and Cartography - Remote Sensing and Geospatial Technologies for Coastal Ecosystem Assessment and Management": Springer Publication pp 365-389.

Figure G.2: Harding, D.J., 2009, Pulsed laser altimeter ranging techniques and implications for terrain mapping, in Topographic Laser Ranging and Scanning: Principles and Processing, Jie Shan and Charles Toth, eds., CRC Press, Taylor & Francis Group, pp. 173-194

Figure G.3: Leveson, Irving, 2006, Benefits of the New GPS Civil Signal – The L2C Study, *InsideGNSS* July/August 2006 (http://www.insidegnss.com).

Figure G.4: http://www.ngs.noaa.gov/CORS/ last accessed October 24, 2011.

Figure G.5: Smith, D.A., Roman, D.R., 2010. How NOAA's GRAV-D Project Impacts and Contributes to NOAA Science (http://www.ngs.noaa.gov/grav-d/pubs/GRAV-D_Contribution_to_NOAA_Science.pdf, last accessed September 15, 2011).

IFSAR/InSAR System Technologies

Evaluate the extent to which IFSAR technology could meet enhanced elevation Business Uses in general, and in what geographic areas IFSAR might either be used instead of LiDAR, or as a methodology for updating elevations previously derived from LiDAR data.

Interferometric Synthetic Aperture Radar, abbreviated as IFSAR (also InSAR), is a well-established remote sensing technology for obtaining mid-level accuracy of x, y and z coordinates of a location imaged by two radar beams. IFSAR uses two or more synthetic aperture radar (SAR) complex images, containing amplitude and phase, to generate data used for production of Digital Surface Models (DSMs) and Digital Terrain Models (DTMs), using differences in the phase of the waves returning to the satellite or aircraft. A bi-product of an IFSAR configuration are orthorectified radar images which have been corrected for terrain distortions.

Differential InSAR (DInSAR) maps changes in elevations (due to subsidence, volcanic activity, an earthquake or other changes) using differences in interferograms collected at different dates and topographic heights. An important aspect of DInSAR is to remove topographic height information so that the elevation changes reflect pre/post temporal changes. DInSAR can potentially measure relative elevation changes at the centimeter-scale over timespans of days to years, subject to the availability of data. It has applications for geophysical monitoring of natural hazards, for example earthquakes, volcanoes and landslides, and is effective in monitoring of changing water levels and subsidence. However, it is not very effective in monitoring changes to vegetation.

SAR/IFSAR/InSAR Tutorial

This tutorial includes information from two primary sources:

- The 2nd edition of "Digital Elevation Model Technologies and Applications: The DEM Users Manual," published in 2007 by the American Society for Photogrammetry and Remote Sensing (ASPRS) edited by David Maune of Dewberry; the chapter authors are Scott Hensley and Paul Rosen from the Jet Propulsion Laboratory (JPL) and Riadh Munjy from the California State University, Fresno.
- A paper prepared for Dewberry by Lorraine Tighe of Intermap Technologies, Inc., entitled: "Elevation Data for United States – IFSAR Option."

Frequency Bands

Synthetic aperture radar (SAR) systems are currently operating over a wide range of frequencies and resolutions depending on their intended applications. Operating frequencies vary from as low as 3 MHz to as high as 40 GHz. The choice of frequency is dictated by a number of factors including intended application, platform and power constraints, and availability of the desired frequency range. Table G.1 shows the correspondence between frequency, wavelength and the band designation letter code (assigned in World War II for security reasons) that are often used to specify the operating frequency of the radar. For the purpose of this assessment, we are primarily interested in the X-, C-, L- and P-bands, listed in order of increasing wavelength.

Table G.1. Frequency and Wavelength Relationship Table

Frequency Band (GHz)	Wavelength Range (cm)	Band Identification
26.5 – 40	1.13 – 0.75	Ka
18 – 26.5	1.66 – 1.13	K
12.5 – 18	2.4 – 1.66	Ku
8 – 12.5	3.75 – 2.4	X
4 – 8	7.5 – 3.75	C
2 – 4	15 – 7.5	S
1 – 2	30 – 15	L
0.3 – 0.9	100 – 33	P or UHF
0.03 – 0.3	1,000 – 100	VHF
0.003 – 0.03	10,000 – 1,000	HF

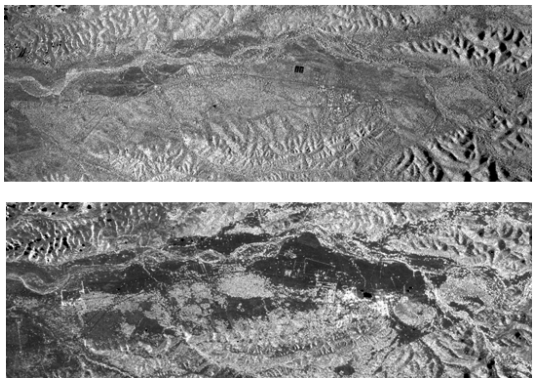

GeoSAR is a commercially-available airborne IFSAR system that acquires both X-band and P-band data. Figure G.6 demonstrates differences between these two bands.

Figure G.6. GeoSAR X-band (top) and P-band (bottom) orthorectified SAR image of Hunter Liggett. Notice how the vegetated areas in the center portion of the image have much greater contrast at P-band (85 cm wavelength) than X-band (3 cm wavelength). This contrast differential results from open areas appearing smoother at P-band than X-band whereas the vegetated areas appear rough at both wavelengths. C- and L-band IFSAR also have advantages and disadvantages. [Image from ASPRS *DEM Users Manual*, 2007.]

Phase Differences

IFSAR is a comparison of two or more coherent SAR images collected at slightly different geometries. The IFSAR process extracts phase differences caused by changes in the elevation within the scene relative to a reference point. Digital elevation information about the Earth's surface is derived from the phase content of two radar signals through IFSAR techniques. The basic idea is that the height of a point on the Earth's surface can be reconstructed from the phase difference between two signals arriving at two antennae housed in a radome. This is because the phase difference is directly related to the difference in path lengths traversed by the signal between the point on the Earth surface and the two antennae. The outcome is an orthorectified radar image (ORI) and DSM which can then be used to derive a DTM. IFSAR systems rely on picking up the radar return signal using antennae at two different locations (see Figure G.7). Each antenna collects amplitude and phase data independently of the other, and the images each receives are almost identical, except for the almost insignificant difference in their range to any specific target. In other words, there is no appreciable

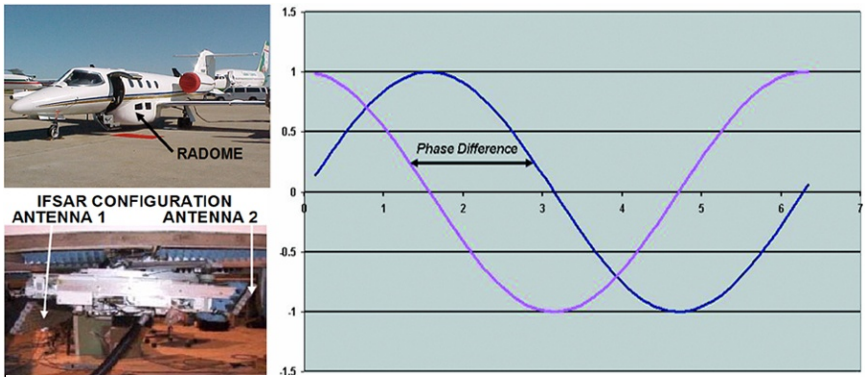

Figure G.7. IFSAR configuration with two antennae in the radome (left); schematic of two identical waves that are out of phase (right).

separation (parallax) between the images. With IFSAR the patterns of electromagnetic radiation (light waves) emanating from the same point on the ground strike each antenna independently. This is because they are at slightly different ranges (locations) due to the separation of the antennae. Consequently, these waves do not always overlap each other exactly and are said to be out of phase by some amount. This is called a phase difference, as shown at Figure G.7. The waves that are received at antenna 1 shift in and out of phase with respect to those received at antenna 2, depending on where the point is located from which they are being reflected.

High interferometric correlation is desired for accurate elevation data. Interferometric correlation, a measure of the similarity of the signal received at the two antennas, can be estimated directly from the image data of the two interferometric channels. Correlation measurements have values between 0 and 1, with 1 designating perfect correlation between the channels. Sometimes it is more convenient to refer to the amount of interferometric decorrelation, which is defined as one minus the correlation. The amount of decorrelation due to the slightly different viewing geometry is called geometric decorrelation. Thermal noise induced signal decorrelation is called noise decorrelation. Shadowed regions suffer from noise decorrelation and areas on steep slopes exhibit geometric decorrelation that increases phase noise and can preclude useful phase measurements altogether.

Polarization

Radar waves have a polarization. Different materials reflect radar waves with different intensities, but anisotropic materials such as grass often reflect different polarizations with different intensities. Some materials will also convert one polarization into another. By emitting a mixture of polarizations and using receiving antennae with a specific polarization, several different images can be collected from the same series of pulses. Frequently three such polarizations (HH, VV, VH), where H is horizontal and V is vertical (the first letter being transmitted; the second letter being received) are used as the three color channels in a synthesized image. This is what has been done in Figure G.8, a polarimetric SAR image of Death Valley colored using three polarizations. Interpretation of the resulting colors requires significant testing of known materials.

Figure G.8. Three SAR polarization bands in Death Valley, CA.

New developments in polarimetry also include utilizing the changes in the random polarization returns of some surfaces (such as grass or sand), between two images of the same location at different points in time to determine where changes not visible to optical systems occurred. Examples include subterranean tunneling or paths of vehicles driving through the area being imaged. Enhanced SAR sea oil slick observation have been developed by appropriate physical modeling and use of fully-polarimetric and dual-polarimetric measurements.

Sample IFSAR Sensor Configurations and Specifications

Table G.2 Summarizes key parameters of some of the SAR systems that may be used to derive elevation data via Interferometric methods.

Table G.2. Key parameters of some SAR systems used to derive elevation data via Interferometric methods.

	Airborne Sensors		Satellite Sensors				
Sensor	**STAR-NEXTMap**	**GeoSAR**	**Tandem-X**	**COSMO-SkyMed**	**SRTM**	**RADARSAT II**	**ALOS**
Country	**Canada**	**USA**	**Germany**	**Italy**	**USA**	**Canada**	**Japan**
Frequency	9.6 GHz	10GHz-X; 353 MHz-P	9.6 GHz	9.6 GHz	5.6 GHz	5.3 GHz	
Wavelength	X	X and P	X	X	C	C	L
Polarization	HH	X-HH & P-VV/HH	HH, VV, HV, VH	HH, VV, HV, VH	HH	HH, VV, HV,	HH, VV, HV,
InSAR Operation Mode	Single-pass	Single-pass	Repeat-pass	Repeat-pass	Single-pass	Repeat-pass	Repeat-pass
Cross-Range Resolution	.625 - 1.25m	1-3m	3-10m	3-10m	30m	3-50m	30m
Elevation Product	DSM/DTM	DSM/DTM	RAW Data	RAW Data	DSM	Raw Data	Raw Data
Post Spacing	5m	3m (X) 5m (P)	5m	15-30m	30m/90m	20m	30m
Hydro Enforced	Yes (3D)	Yes (2D)	No	No	Yes (3D)	No	No
Revaltive Vertical Accuracy	50cm-3m rms	2-5m rms (X) 5-10m rms(P)	10m rms	10m rms	16m rms	15-30m rms	10-20m rms
Imagery Product	ORI - X	ORI X/P	RAW - X	No	No	No	No
Imagery Resolution	.625 m - 2.5m	1.25 & 3	3	N/A	N/A	3	N/A
X-Y Accuracy (m CE)	2	?	5	3 m	16m RMSE	5	10 m
Repeat Cycle	N/A	N/A	11 days	1 day	Once	24 days	46 days
Swath Width	10 km	20 km	30 km	40 km	60km	20 km	40-70 km
YEAR	1997-ongoing	>2000	>2010	2007	2000	2007	2006
DEM Data Archive	Yes	No	No	No	Yes	No	No

As shown in this table, in addition to airborne STAR and GeoSAR sensors, there are other IFSAR/InSAR satellites in operation today. Table G.2 provides a sample of satellite IFSAR (InSAR) sensors, but there are others, including the ENVISAT (C-band), Radarsat-1 (C-band) and the JERS (L-band).

For production of DSMs and DTMs, the wavelength largely controls the vertical accuracy achievable and the resolution of image and elevation products. Much research has been performed into the relative merits of X-band, C-band, L-band, and P-band. One such study compared the L-band data from ALOS PALSAR with the C-band data from Envisat, and concluded that the longer wavelength data from L-band can be used to resolve deformations with greater phase gradients and has better coherence than C-band for post-earthquake analyses. In many cases, the repeat pass frequency is paramount.

SAR resolution is determined in the range and azimuth directions independently of each other. Real aperture radar azimuth resolution is determined by the ratio of the wavelength of light being observed to the length of the aperture being used to collect it. The larger the aperture, the better the resolution of the data will be. However, in the case of SAR, a synthetic aperture and the forward motion of the platform carrying the SAR sensor are used to create a narrow beam width from the SAR antenna, resulting in a long synthetic aperture which yields a finer azimuth resolution than is possible from a smaller physical antenna. Range resolution is directly proportional to the pulse length such that high resolution requires short pulses or high intensities. Fortunately with SARs, signal processing techniques

have been developed to use an extended pulse at lower intensities and lower power to still achieve fine resolution.

The major advantage of all IFSAR bands, however, is that they are (nearly) all-weather, penetrating clouds and fog that prevent acquisition of usable elevation data by optical sensors from LiDAR and photogrammetry. Like LiDAR, IFSAR also operates at night time which cannot be done with optical imagery for photogrammetry. A second major advantage is that it is less expensive for wide-area acquisition than LiDAR or photogrammetric DTMs, but absolute accuracies are typically not as good. Relative accuracies from satellite- and airborne-based IFSAR systems, on the other hand, can be extremely good, enabling a variety of vertical change detection applications (i.e., detection of small vertical displacements), as described below.

SAR applications that generate only an image make use of the amplitude and phase, where the end product contains only the amplitude. However interferometry uses the phase of the reflected radiation. Since the outgoing wave is produced by the active satellite or airborne sensor, the phase is known, and can be compared to the phase of the return signal. The phase of the return wave depends on the distance to the ground, since the path length to the ground and back will consist of a number of whole wavelengths plus some fraction of a wavelength. This is observable as a phase difference or phase shift in the returning wave. The total distance to the satellite or aircraft (i.e. the number of whole wavelengths) is not known, but the extra fraction of a wavelength can be measured extremely accurately. This phase difference information can generate high resolution elevation data.

Factors affecting phase in the IFSAR technique

The most important factor affecting the phase is the interaction with the ground surface. The phase of the wave may change on reflection, depending on the dielectric or structural properties of the material. The reflected signal back from any one pixel is the summed contribution to the phase from many smaller 'targets' in that ground area, each with different dielectric and structural properties and distances from the IFSAR platform, meaning the returned signal is arbitrary and completely uncorrelated with that from adjacent pixels (a phenomenon known as constructive and deconstructive interference). Importantly though, it is consistent - provided nothing on the ground changes the contributions from each target (e.g., non-temporal decorrelation in phase) should sum identically each time, and hence be removed from the interferogram.

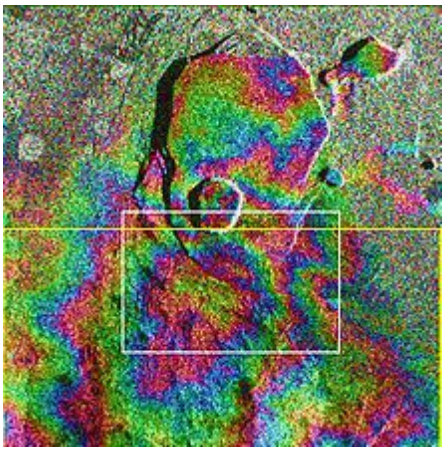

Figure G.9. Interferogram of Kilauea, HI showing topographic fringes (NASA/JPL-Caltech)

Once the ground effects have been removed (typically by filtering), the major signal present in the interferogram is a contribution from platform effects. For example, for spaceborne interferometry to work, the satellites must be as close as possible to the same spatial position when the images are acquired. This means that images from two different satellite platforms with different orbits cannot be compared, and for a given satellite data from the same orbital track must be used. In practice the perpendicular distance between them, known as the

interferometric baseline, is often known to within a few centimeters but can only be controlled on a scale of tens to hundreds of meters. This slight difference causes a regular difference in phase that changes smoothly across the interferogram and can be modeled and removed (Figure G.9).

The slight difference in satellite position also alters the distortion caused by topography, meaning an extra phase difference is introduced by a stereoscopic effect. The longer the *interferometric baseline*, the smaller the topographic height needed to produce a fringe of phase change - known as the *altitude of ambiguity*. This effect can be exploited to calculate the topographic height, and used to produce a digital surface model (DSM).

If the height of the topography is already known, the topographic phase contribution can be calculated and removed. This has traditionally been done in two ways. In the *two-pass* method, elevation data from an externally-derived DEM is used in conjunction with the orbital information to calculate the phase contribution. In the *three-pass* method two images acquired a short time apart are used to create an interferogram, which is assumed to have no deformation signal and therefore represent the topographic contribution. This interferogram is then subtracted from a third image with a longer time separation to give the residual phase due to deformation, rather than topographic height.

Once the ground, orbital and topographic contributions have been removed, the interferogram contains the deformation signal, along with any remaining noise. The signal measured in the interferogram represents the change in phase caused by an increase or decrease in distance from the ground pixel to the satellite, therefore only the component of the ground motion parallel to the satellite line of sight vector will cause a phase difference to be observed. For sensors like ERS with a small incidence angle this measures vertical motion well but is insensitive to horizontal motion perpendicular to the line of sight (approximately north-south). It also means that vertical motion and components of horizontal motion parallel to the plane of the line of sight (approximately east-west) cannot be separately resolved.

One fringe of phase difference is generated by a ground motion of half the radar wavelength, since this corresponds to a whole wavelength increase in the two-way travel distance. Phase shifts are only resolvable relative to other points in the interferogram. Absolute deformation can be inferred by assuming one area in the interferogram (for example a point away from expected deformation sources) experienced no deformation, or by using ground control (GPS or similar) to establish the absolute movement of a point.

Satellite-based IFSAR Challenges

Currently, the Astrium Tandem-X satellite system is the only true IFSAR configuration in space. However, a variety of other space platforms are available for repeat-pass IFSAR image data collection (Table G.2). A variety of factors govern the choice of images which can be used for repeat-pass interferometry. The simplest is data availability - radar instruments used for interferometry commonly don't operate continuously, acquiring data only when programmed to do so. For future requirements it may be possible to request acquisition of data, but for many areas of the world archived data may be sparse. Data availability is further constrained by baseline criteria. Availability of a suitable DEM may also be a

factor for two-pass InSAR; commonly 90m SRTM data may be available for many areas, but at high latitudes (e.g., Alaska) or in areas of poor coverage alternative datasets must be found.

A fundamental requirement of the removal of the ground signal is that the sum of phase contributions from the individual targets within the pixel remains constant between the two images and is completely removed. However there are several factors that can cause this criterion to fail. Firstly the two images must be accurately co-registered to a sub-pixel level to ensure that the same ground targets are contributing to that pixel. There is also a geometric constraint on the maximum length of the baseline - the difference in viewing angles must not cause phase to change over the width of one pixel by more than a wavelength. The effects of topography also influence the condition, and baselines need to be shorter if terrain gradients are high. Where co-registration is poor or the maximum baseline is exceeded the pixel phase will become incoherent - the phase becomes essentially random from pixel to pixel rather than varying smoothly, and the area appears noisy. This is also true for anything else that changes the contributions to the phase within each pixel, for example, changes to the ground targets in each pixel caused by vegetation growth, landslides, agriculture or snow cover.

Another source of error present in most interferograms is caused by the propagation of the waves through the atmosphere. If the wave travelled through a vacuum it should theoretically be possible (subject to sufficient accuracy of timing) to use the two-way travel-time of the wave in combination with the phase to calculate the exact distance to the ground. However the velocity of the wave through the atmosphere is lower than the speed of light in a vacuum, and depends on air temperature, pressure and the partial pressure of water vapor. It is this unknown phase delay that prevents the integer number of wavelengths being calculated. If the atmosphere was horizontally homogeneous over the length scale of an interferogram and vertically over that of the topography, then the effect would simply be a constant phase difference between the two images which, since phase difference is measured relative to other points in the interferogram, would not contribute to the signal. However the atmosphere is laterally heterogeneous on length scales both larger and smaller than typical deformation signals. This spurious signal can appear completely unrelated to the surface features of the image, however in other cases the atmospheric phase delay is caused by vertical heterogeneity at low altitudes and this may result in fringes appearing to correspond with the topography.

Producing interferograms

The processing chain used to produce interferograms varies according to the software used and the precise application, but will usually include some combination of the following steps.

Two SAR images are required to produce an interferogram; these may be obtained pre-processed, or produced from raw data by the user prior to IFSAR processing. The two images must first be co-registered, using a correlation procedure to find the offset and difference in geometry between the two amplitude images. One SAR image is then re-sampled to match the geometry of the other, meaning each pixel represents the same ground area in both images. The interferogram is then formed by cross-multiplication of each pixel in the two images, and the interferometric phase due to the curvature of the Earth is removed, a process referred to as earth flattening.

Once the basic interferogram has been produced, it is commonly filtered using an adaptive power-spectrum filter to amplify the phase signal. For all quantitative applications the consecutive fringes present in the interferogram will then have to be *unwrapped*, which involves interpolating over the 0 to 2π phase jumps to produce a continuous elevation surface. At some point, before or after unwrapping, incoherent areas of the image may be masked out. The final processing stage involves geocoding the image, which resamples the interferogram from the acquisition geometry (related to direction of platform path) into the desired geographic projection.

Airborne IFSAR application

Airborne IFSAR, widely used for topographic mapping, produces DSMs and DTMs with vertical accuracies between 10-foot and 20-foot equivalent contour accuracies (RMSEz between 3 and 6 feet). Table G.3 identifies federal government agencies and an NGO that specified mission-critical requirements for airborne IFSAR data for Business Uses and Functional Activities. Many of the requirements specified for Alaska in this table reflect agencies that may need or prefer LiDAR data, but specified IFSAR, recognizing technical and/or cost issues in acquiring LiDAR in Alaska due to weather constraints. Alaska experiences extensive cloud and fog conditions where LiDAR would be successful only under ideal conditions that generally do not prevail or are hard to predict. Therefore, the entire state of Alaska is considered to be a geographic area where it makes common sense for IFSAR to be used instead of LiDAR, except for smaller mission-specific projects. Details are provided in Appendices B through E.

Table G.3. Business Uses and Functional Activities with requirements for airborne IFSAR, including Alaska where IFSAR is recognized as the only viable alternative for vast wilderness areas with frequent cloud cover and fog.

Business Uses	User Organization	Functional Activity	Geographic Area
1,2,6	NRCS	Conservation Engineering and Practices	Western mountains plus Alaska[11]
1	NRCS	Specialized Mapping Applications	Alaska[7]
1,9	USFS	Soil and Geology Inventory	Alaska[7]
1	USFS	Wetlands Mapping and Characterization	Alaska[7]
1	EPA	Environmental Protection, Land Cover Characterization, Runoff Modeling	Alaska[7]
1, 13	NPS	Preservation and Protection of Natural and Cultural Resources	Alaska[7]
2	USFS	Watershed Analysis	Alaska[7]
2, 23	EPA	Broad Area Air and Water Quality Research	Nationwide
4	NOAA	Coastal Mapping and Modeling	Coastal states
5	USFS	Forest Inventory and Assessment	Alaska[7]
7	FWS	National Wildlife Refuge System	Alaska[7]
7	FWS	Endangered Species and Fisheries and Habitat Conservation	Alaska[7]
7	FWS	Migratory Birds	Alaska[7]
11	NextEra Energy	Wind Farm Siting and Design	Nationwide
12	Anonymous Oil & Gas Company	Oil and Gas Operations	Alaska[7]

[11] All geographic areas that state Alaska[7] are agencies that would prefer LiDAR data but will settle for IFSAR in recognition of the limitations of LiDAR in cloud and fog-covered areas of Alaska where LiDAR cannot be reliably acquired.

14	FEMA	Flood Risk Analysis	Areas of low flood risks
14	NOAA	Advanced Hydrologic Prediction Service Static Inundation Mapping	Western areas and Alaska
16	USFS	Wildfire Management	Alaska[7]
16	BLM	Wildland Firefighting	Alaska[7]
18,26	TomTom	In-Car Location and Navigation Products & Services	Alaska[7]
20	FAA	Enroute Instrument Procedure Development	Nationwide
20	e-Terra	Alaska Aviation Safety Project	Alaska[7]
21	USFS	Infrastructure Management	Alaska[7]
23	CDC	Human, Animal and Environmental Health	Alaska[7]
25	NASA	Advanced Earth Science Mission	Alaska[7]
27	FCC	Spectrum Management and Frequency Coordination	Nationwide

Satellite IFSAR (InSAR) and Differential InSAR (DInSAR)

Satellite InSAR produces DSMs with vertical accuracies between 30-foot and 50-foot contour accuracies (RMSEz between 9 and 15 feet). Few commercial vendors generate satellite derived DTMs. The greatest interest in satellite InSAR was from differential InSAR (DInSAR) which measures precise relative changes in elevation, over time, to assess areas of subsidence, earthquake movement, volcanic activity, or a flood event, for example, to the centimeter or even millimeter level. Table G.4 identifies federal government agencies that specified mission-critical requirements for satellite DInSAR data for Business Uses and Functional Activities listed.

Table G.4. Business Uses and Functional Activities with requirements for satellite differential InSAR (DInSAR)

Business Uses	User Organization	Functional Activity	Geographic Area
1,7	FWS	Wetland Inventory and Mapping	Nationwide
23	CDC	Waterborne Disease Prevention	Nationwide

DInSAR for detection of changes in water surface elevations

The two Functional Activities in Table G.4 identify requirements for repeat-pass DInSAR where satellite DInSAR offers better potential for accurately detecting small changes in water surface elevations than does airborne DInSAR because of the ability of satellites to precisely duplicate their orbits with repeat passes and achieve correlation between interferograms acquired on different dates.

The Fish and Wildlife Service initially asked for IFSAR based on successes in the Florida Everglades, documented in the February 2010 issue of *IEEE Transactions on Geoscience and Remote Sensing*, Vol. 48, No. 2. The authors (Sang-Hoon Hong and Shimon Wdowinski from the University of Miami, and Sang-Wan Kim from Sejong University, Korea) authored an article entitled: "Evaluation of TerraSAR-X Observations for Wetland InSAR Application." In this paper, the authors explored the feasibility of X-band TerraSAR-X (TSX) data for the wetland InSAR application. Their analysis demonstrated "that X-band InSAR works quite well in wetlands and can be used for monitoring water-level changes in this challenging environment."

A credible analysis was ideal in the Florida Everglades where the surface water levels are monitored by probably the densest stage (water level) network in the world, consisting of more than 200 stations, spaced 5-10 km from one another. This very wide flow combined with the dense state network provided

an almost perfect large-scale natural and controlled laboratory for testing space-geodetic hydrological technologies. Two study areas were used:

- The northern study area consisted of two TSX consecutive frames. This study area was selected because it contains both wetland and urban environments, allowing the researchers to compare the interferometric phase and coherence calculated for the two environments. The wetlands in this section of the Everglades are divided by a set of levees into five managed areas: Water Conservation Areas (WCA) 1, 2A, 2B, 3A and 3B; these areas serve as water reservoirs for the large southeast Florida populations. The southwestern corner of the northern study area was comprised of natural-flow wetlands which are parts of the Everglades National Park (ENP).
- The southern study area is located within the ENP across the transition between freshwater and saltwater (mangrove) wetlands. This area was selected to evaluate the suitability of the wetland InSAR application in different wetland environments, including woody (saltwater mangrove) and herbaceous (freshwater) vegetations. Furthermore, the researchers' previous L-band study showed detectable water-level changes (fringes) across this transition induced by tide movement in the saltwater mangrove. Thus the researchers expected to find tide-induced water-level changes in this area.

The researchers processed the TSX data with the Repeat Orbit Interferometry PACkage software, which calculates repeat-pass interferograms using a digital elevation model (DEM) to eliminate topographic effects. After confirming that TSX HH polarization data are suitable for InSAR wetland applications, the team performed a multipolarization study to explore the suitability of other polarization-data types to this application, acquiring dual-polarization data in the two study areas and experimenting with different polarization pairs: HH/HV, VV/VH, and HH/VV. The main goal was using the phase data to calculate different polarization interferograms. The interferograms showed that phase is maintained in almost all wetland areas. They found that the coherence in urban areas is significantly higher than in wetlands with all combinations of polarization pairs.

The team concluded: "The most important outcome of this study was the surprising result that wetland InSAR works well with X-band TSX data. The advantages of the TSX data are the following: very high pixel resolution (1-3 m), short repeat orbit interval (11 days), data acquisition with different polarization parameters, and high detection level reflecting the 3.1 cm wavelength of the TSX radar system. These properties can be very useful for monitoring detailed flow patterns, such as the effect of channels as conduits in wetlands. The disadvantages of the TSX data are the following: small coverage area (10-30-km-wide swath) and possible fringe saturation in areas with high gradient of water-level changes. These limitations of the TSX system suggest that TSX data should not be used in the same way as the wider swath C- and L-band systems, which cover large wetland areas. The very high resolution TSX data should be used wisely for localized targets that need detailed information, such as the relationships between wetland and channel flow."

These authors also prepared a Power Point presentation entitled "Wetland InSAR over the Everglades from space observed polarimetric data." Two slides from that presentation are shown below. Figure G.10 shows interferograms from C-band and L-band InSAR satellites. Figure G.11 shows how all

polarizations were successful in mapping changes in water surface elevations, but the X-band HH polarization worked the best.

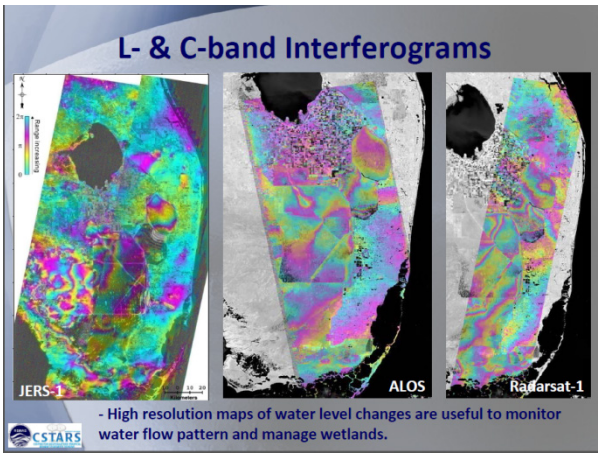

Figure G.10. Satellite DInSAR interferograms map cm-level changes in water levels from different SAR satellites. C-band and L-band systems cover large wetland areas

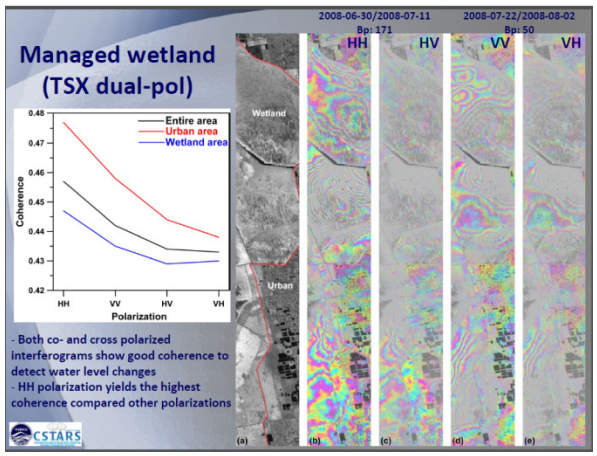

Figure G.11. TerraSAR-X (TSX) HH (horizontal-horizontal) polarization provides the highest coherence to detect water level changes.

DInSAR for detection of changes in topographic surface elevations

Interferometric SAR (InSAR) exploits the phase differences of at least two complex-valued SAR images (containing amplitude and phase) acquired from different orbit positions and/or at different times. Research has shown that the information derived from these interferometric data sets can be used to measure several geophysical quantities, such as topography, deformations (volcanoes, earthquakes, ice fields), and glacier flows.

One such research project was documented in the *Annual Review of Earth and Planetary Sciences*, Vol 28: 169-209 (published in May 2000), authored by Roland Burgmann of the University of California, Berkeley, as well as Paul A. Rosen and Eric Fielding of the Jet Propulsion Laboratory (JPL). The article is entitled: "Synthetic Aperture Radar Interferometry to Measure Earth's Surface Topography and its Deformation." The abstract reads as follows:

> Synthetic aperture radar interferometry (InSAR) from Earth-orbiting spacecraft provides a new tool to map global topography and deformation of the Earth's surface. Radar images taken from slightly different viewing directions allow the construction of digital elevation models of meter-scale accuracy. These data sets aid in the analysis and interpretation of tectonic and volcanic landscapes. If the Earth's surface deformed between two radar image acquisitions, a map of the surface displacement with tens-of-meters resolution and subcentimeter accuracy can be constructed. This review gives a basic overview of InSAR for Earth scientists and presents a selection of geologic applications that demonstrate the unique capabilities of InSAR for mapping the topography and deformation of the Earth.

A second research project documented the use of DInSAR for detection of aquifer system compaction and land subsidence in California. The paper is entitled: "Detection of aquifer system compaction and land subsidence using interferometric synthetic aperture radar, Antelope Valley, Mohave Desert, California. Authored by D. L. Galloway, I.W. Hudnut, S. E. Ingbritsen, and S. P. Phillips of USGS, and G. Peltzer, F. Rogez, and P.A. Rosen of JPL, the abstract reads as follows:

Interferometric synthetic aperture radar (InSAR) has great potential to detect and quantify land subsidence caused by aquifer system compaction. InSAR maps with high spatial detail and resolution of range displacement (610 mm in change of land surface elevation) were developed for a groundwater basin (;103 km2) in Antelope Valley, California, using radar data collected from the ERS-1 satellite. These data allow comprehensive comparison between recent (1993–1995) subsidence patterns and those detected historically (1926–1992) by more traditional methods. The changed subsidence patterns are generally compatible with recent shifts in land and water use. The InSAR-detected patterns are generally consistent with predictions based on a coupled model of groundwater flow and aquifer system compaction. The minor inconsistencies may reflect our imperfect knowledge of the distribution and properties of compressible sediments. When used in conjunction with coincident measurements of groundwater levels and other geologic information, InSAR data may be useful for constraining parameter estimates in simulations of aquifer system compaction.

DInSAR has also been used for mapping of subsidence from underground coal fields. The *Journal of Applied Remote Sensing* (April, 2011), included a paper entitled: "Coal mining induced land subsidence monitoring using multiband spaceborne differential interferometric synthetic aperture radar data" by Huanyin Yue of the National Remote Sensing Center of China; Guang Liu, Huadong Guo and Xinwu Li of the Chinese Academy of Sciences, Center for Earth Observation and Digital Earth;Zhizhong Kang of the China University of Geosciences; Runfeng Wang of the China Hebei Bureau of Surveying and Mapping; and Xuelian Zhong of the Chinese Academy of Sciences, Institute of Electronics. The abstract reads as follows:

The differential Interferometric synthetic aperture radar (SAR) (DInSAR) technique has been applied to the earth surface deformation monitoring in many areas. In this paper, the DInSAR technique is used to process the spaceborne SAR data including C band ENVISAT ASAR, L band JERS SAR, and ALOS PALSAR data to derive the temporal land subsidence information in the Fengfeng coal mine area, Hebei province in China. Since JERS and ALOS do not have precise orbit, an orbit adjustment must be accomplished before the DInSAR interferogram was formed. Twenty-three differential interferograms are derived to show the temporal change of the land subsidence range and position. At the acquisition time of ENVISAT ASAR, the leveling in the Dashucun coal mine in Fengfeng area was carried, the historical excavation data in 8 coal mines in Fengfeng area from 1992 to 2007 were collected as well. In our analysis, the DInSAR results are compared with leveling data and historical excavation data. The comparison results show the DInSAR subsidence results are consistent with the leveling results and the historical excavation data, and the L band DInSAR shows more advantages than C band in the coal mining induced subsidence monitoring in a rural area. The feasibility and limitations in coal mining induced subsidence monitoring with DInSAR are analyzed, and the possibility of underground mining activity monitoring by spaceborne InSAR data is evaluated. The experimental results show that both C and L band can accomplish monitoring mining area subsidence, but C band has more restricted conditions of its perpendicular baseline. In order to get a satisfactory outcome in mining area subsidence by the DInSAR method, the time series of SAR images of every visit and SAR deformation interferograms should be archived.

Similar studies have been performed in the U.S. documenting the application of differential interferometric synthetic aperture radar to identify, measure and analyze subsidence above underground coal mines in Utah.

Alternative IFSAR Uses

Airborne IFSAR systems were evaluated for their ability to satisfy elevation data requirements for Quality Level 4, including the ability of airborne IFSAR to characterize above-ground structures and vegetation characteristics. Very few users specified a need for QL4 data from stereo photogrammetry QL4 covers a broad accuracy range (RMSEz between 46 and 139 cm). Airborne IFSAR could satisfy some QL 4 requirements with an RMSEz between 93 and 139 cm, but not requirements with RMSEz <93 cm.

Airborne IFSAR technology was also evaluated as a methodology for updating elevations previously derived from LiDAR data and prior IFSAR data collects, recognizing that the relative accuracy of IFSAR data is better than its absolute accuracy. Airborne IFSAR could not be used to update elevations previously acquired from LIDAR with 1- to 2-foot contour accuracy, with one exception – in the case where new IFSAR data can identify major changes in topography that occurred after the date of the LiDAR data acquisition. For this scenario, less-accurate IFSAR data would be better than obsolete LiDAR data for the small areas where major changes occurred. Differential IFSAR (DInSAR) does not work well with airborne IFSAR, primarily due to the inaccuracies in determining the positioning of the aircraft, but it does work with satellite InSAR, as described above, which also has limitations. If the bare earth terrain was free of vegetation for the initial collect and follow-on collect, then DInSAR should work to identify changes. However, neither airborne DInSAR nor satellite DInSAR work well in vegetated terrain.

Intermap's NEXTMap® USA QL5 IFSAR data are already available nationwide for 49 of the 50 states (all except Alaska) and are superior (in terms of resolution, accuracy and currency) to most of the elevation data currently in the NED where LiDAR has not been collected. Whereas it has previously licensed NEXTMap® USA data, new management at Intermap Technologies Inc. is now receptive to the idea of licensing the data (gridded DTMs, DSMs and ORIs) to USGS for public dissemination via the NED. Figures G.12 through G.19 compare NEXTMap® USA data with the NED in selected areas.

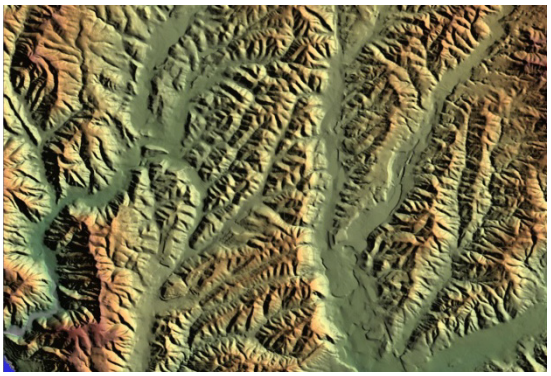

Figure G.12. San Juan Capistrano, CA NED

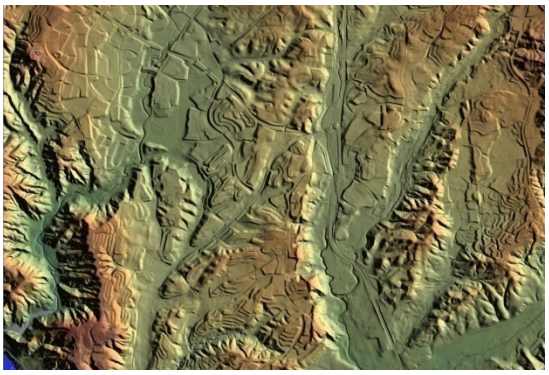

Figure G.13. San Juan Capistrano, CA NEXTMap® USA IFSAR

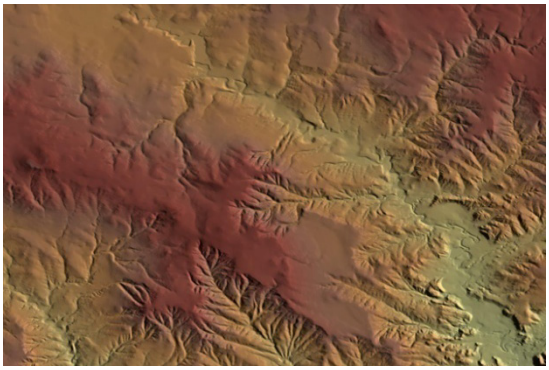

Figure G.14. Tecla, WY NED

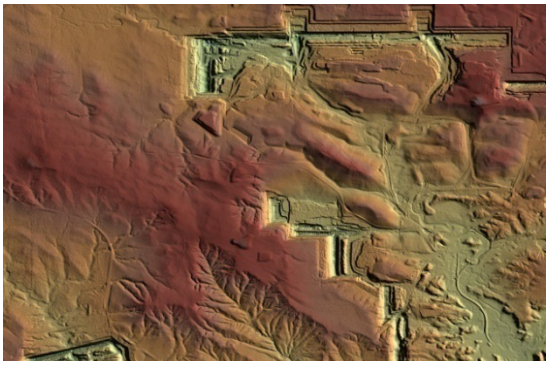

Figure G.15. Tecla, WY NEXTMap® USA IFSAR

Figure G.16. Dana Point, CA NED

Figure G.17. Dana Point, CA NEXTMap® USA IFSAR

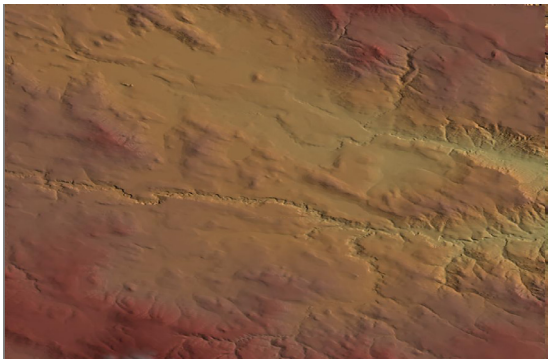

Figure G.18. Reno, NV Reservoir NED

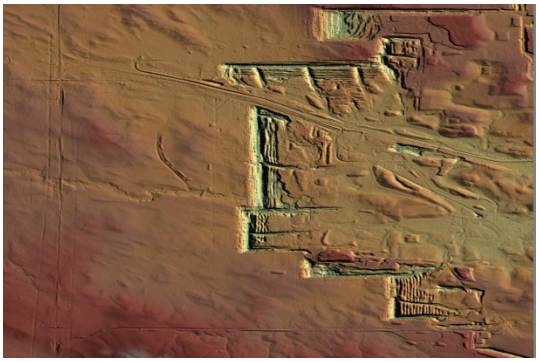

Figure G.19. Reno, NV Reservoir NEXTMap® USA IFSAR

IFSAR/InSAR Technology Conclusions

- IFSAR data (satellite or airborne) lack the resolution and accuracy required to satisfy most Business Use requirements for the NEEA, and hence is not considered a viable solution for obtaining QL1 – QL4 data.
- In Alaska, where clouds and fog severely limit the acquisition of LiDAR and optical imagery, airborne IFSAR is superior due to its ability to map through clouds and fog; it is also superior in Alaska because it maps large, remote areas at relatively low costs.
- Airborne IFSAR is normally ill-suited for updating elevations previously derived from LiDAR data because it has poorer accuracy, poorer resolution and (normally) poorer currency; the one scenario where IFSAR could update LiDAR data is when new IFSAR data are more current than old LiDAR data and could depict topographic changes, such as shown in Figures G.12 through G.19 above.
- Satellite DInSAR offers potential for mapping changes in water surface elevations – something that airborne IFSAR cannot do well.

Coastal Zone Technologies

Research new instrumentation and software advancements to improve the quality and efficiency of bathymetric and topobathymetric LiDAR technology. This research into recent and forthcoming technology advances should cover Federal laboratories (e.g., JALBTCX), industry providers of bathymetric LiDAR instruments (e.g., Optech) and academic institutions (e.g., the University of New Hampshire).

The concept of airborne LiDAR bathymetry (also called bathy LiDAR) grew out of efforts in the 1960's when the newly invented laser was used to detect submarines. As applied to civilian mapping applications, the history of this technology can be traced back to feasibility studies and laboratory prototypes in the late 1960's, and early experimental systems, such as the NASA Airborne Oceanographic LiDAR (AOL) in the 1970's. The primary applications of bathy LiDAR include nautical charting, port and harbor surveys, coastal zone mapping, and military applications. Based on many years of operations, bathy LiDAR has proven to be an accurate, cost-effective, rapid, safe, and flexible method for surveying in shallow water and on coastlines where sonar systems are less efficient and can even be dangerous to operate (Figure G.20). The biggest limiting factor for bathy LiDAR is water clarity and operational depth. As a result, airborne LiDAR bathymetry and ship-based acoustic technologies often complement each other in mapping coastal and marine environments.

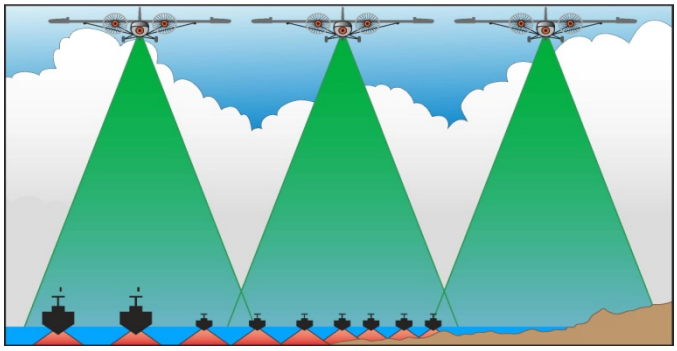

Figure G.20. Depiction of LiDAR and multi-beam sonar operations in shallow water to emphasize LiDAR capabilities and efficiency. [Source: Guenther, 2007]

The first-generation airborne LiDAR systems were successfully developed and tested by the U.S. Navy and NASA. However, much of the technical evolution in bathymetric (hereafter "bathy") and topographic-bathymetric (hereafter "topo-bathy") LiDAR has occurred within the past decade, and we appear to still be on the steep part of the technological growth curve. As with topographic LiDAR, a great leap forward occurred in the 1990s with the rapid advancement of integrated GPS/IMU systems that enabled high-accuracy direct georeferencing. For a number of years, other enhancements were aimed primarily at mapping deeper waters, increasing acquisition efficiency, and automation. Current progress in bathy and topo-bathy LiDAR, on the other hand, appears to be proceeding simultaneously in many different, and less predictable, directions. This is arguably the result of a growing realization that the customer base for bathy and topo-bathy LiDAR extends far beyond the hydrographic surveying/nautical charting community to coastal scientists and geomorphologists studying coastal change, coastal managers, the riverine mapping community, inundation and storm surge modeling communities, coral ecosystem management and conservation groups, and a host of others. Many of these somewhat "non-traditional" users of bathy LiDAR are not concerned with surveying relatively deep (e.g., 10-60 m) waters to International Hydrographic Organization (IHO) standards, but, rather, efficiently mapping very shallow coastal and inland waters for a wide variety of science, modeling, and management applications. That said, the hydrographic surveying community remains a primary driver

of the technology, and many other current advancements are aimed at better meeting hydrographic surveying needs, including object detection and the ability to survey more turbid waters. The following sections describe some of the current and anticipated advancements in bathy and topo-bathy LiDAR, including those aimed at the more traditional, as well as the non-traditional, users of the technology.

Topo-bathy sensor technology and trends

Advances in airborne LiDAR bathymetry have traditionally focused on the ability to map submerged topography in deeper and more turbid waters by increasing the power of the outgoing pulse. However, in order to achieve eye-safe operation with sufficient pulse energy to provide reasonable signal-to-noise ratios, the outgoing beam in bathy LiDARs is purposely expanded to a diameter of at least several meters at the water surface, and the resulting scattering from particulate matter in the water column results in a very wide laser footprint. The resulting net expansion in irradiated bottom area is detrimental to the horizontal and vertical accuracy when very high-relief features are present. Further, the long and wide outgoing laser pulse precludes the ability to separate a reflection from the water surface and a shallow seabed return, thereby creating a limit to the minimum operational depth.

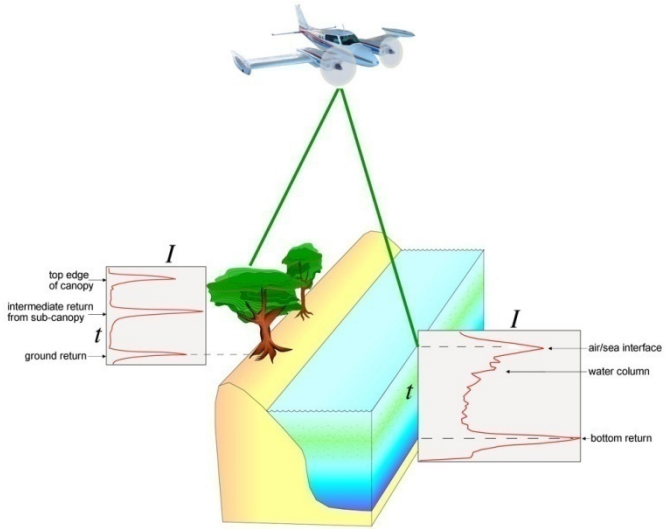

Figure G.21. Topo-bathy LiDAR systems can be used in coastal regions to determine submerged topography and adjacent coastal land elevations in a single scan of transmitted laser pulses, as demonstrated in this conceptual image. The received waveform of energy (I) as a function of time (t) can provide information of vegetated canopies as well as the reflections through water [Source: Nayegandhi et al, 2010].

Instead of focusing on maximum penetrable depth, a new generation of topo-bathy sensors is now focusing on mapping land topography and offshore bathymetry in very shallow coastal and riverine environments (Figure G.21). The design configuration of these systems includes a relatively low-power laser pulse (compared to traditional bathy LiDARs), a narrow transmitted beam, and a small receiver field-of-view. These design characteristics are very similar to topographic LiDAR systems, with the exception that topo-bathy systems use a green-wavelength laser which is able to measure beneath the water surface. A few topo-bathy systems currently being developed use a "beam-splitting and segmented-detector" approach, which divides the outgoing pulse into smaller beamlets and detects the individual beamlets using a segmented detector, thereby maintaining an eye safe operation but still having the ability to measure in deeper and more turbid waters. The size and power requirements of these new topo-bathy systems have also reduced significantly, thereby making the airborne sensor platform-independent and allowing the use of any aircraft-of-opportunity. As laser ranging technology, supporting electronics, and system hardware have developed, the traditional bathy LiDAR systems are being complemented by these high-pulse rate, low power, topo-bathy LiDAR systems. A few of these research and operational systems are described below.

EAARL

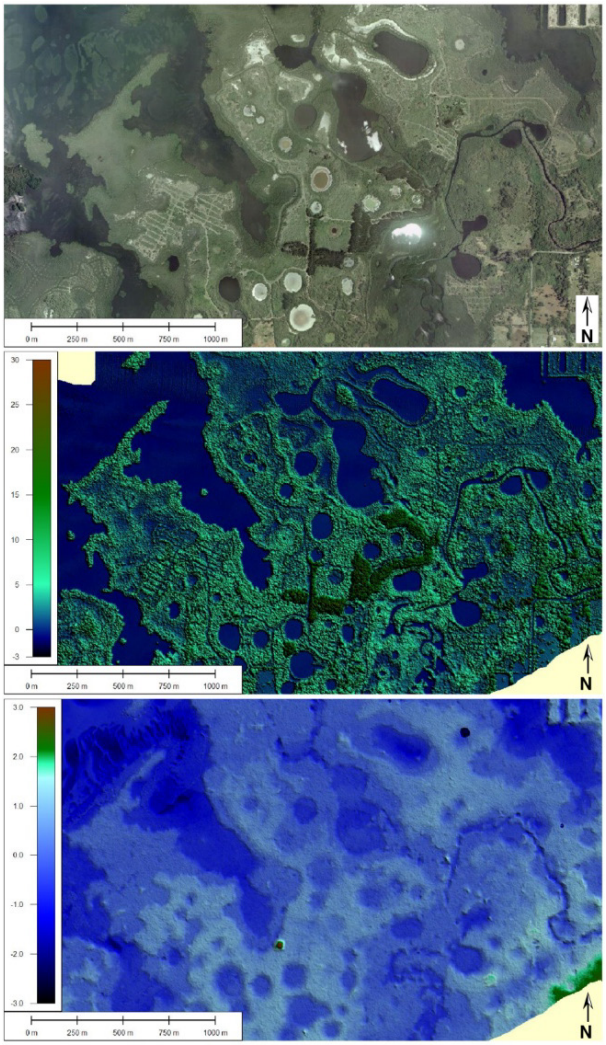

Figure G.22. Coastal-vegetation topography acquired by the EAARL system in Terra Ceia Aquatic and Buffer Preserve, located in the southeast coast of Tampa Bay, FL, USA. (a) High-resolution digital georeferenced imagery of a section of the Preserve shows patches of vegetated communities dominated by invasive species such as Australian pine, Brazilian pepper, and needle grass. Native mangroves surround the many fresh and saltwater ponds in the region. The submerged vegetation is primarily composed of seagrass on sandy substrates. *Image courtesy of TerraServer-USA, obtained using Global Mapper software.* (b) Canopy height sub-aerial topography derived from data acquired by the EAARL system. (c) Seamless topo-bathy DEM acquired by the EAARL system. [Source: Nayegandhi & Brock, 2008].

The USGS Experimental Advanced Airborne Research LiDAR (EAARL, originally developed in 2001 at NASA Wallops Flight Facility, MD) was specifically designed to measure submerged topography and coastal land elevations seamlessly and address some of the challenges that are encountered by traditional bathymetric LiDARs in mapping nearshore coastal environments (Figure G.22). EAARL uses a very low-power, eye-safe laser pulse (in comparison to a traditional bathymetric LiDAR system) that allows for a much higher pulse-repetition frequency and significantly less laser energy per pulse (approximately 1/70th) than do most bathymetric LiDARs. The short pulse width (~1.6 ns full width at half maximum(FWHM)) and small beam divergence (< 2 mrad at nominal flying height of 300 m above ground level) rejects ambient light and multiple-scattered photons from the water column and bottom-reflected backscatter, thereby ensuring relatively high contrast and short duration of the bottom return signal.

The EAARL sensor, owned and operated by the USGS St. Petersburg Coastal and Marine Science Center, is currently being upgraded to improve measurement of bathymetry in shallow and turbid water environments. Enhancements include a more powerful laser with a higher pulse frequency (10 KHz) and shorter pulse width (0.7 ns FWHM), an integrated GPS-INS receiver and a high-speed multichannel waveform digitizer offering 12-bit resolution. The new laser offers up to 400 µJ of pulse power, which is a 500% increase from the original configuration. In order to maintain eye-safe operation, the outgoing pulse is optically segmented into 3 “beamlets”, thereby eliminating the need to spread the outgoing beam and widen the footprint of the laser pulse. The beamlets will also effectively increase the point density to 30 KHz for shallow bathymetric and topographic mapping. Upgrades to the receiver electronics will include three multi-channel waveform digitizers that detect laser backscatter from the three beamlets, and a fourth detector that encompasses the field of view of

the entire outgoing pulse, thereby enabling the ability to map in deeper and more turbid waters. This unique design philosophy of the EAARL-B system is expected to produce greater data density, better water penetration, improved ability to discriminate water surface reflections from bed reflections, better overall accuracy, and better spatial resolution of small topographic features. New software methods will also be implemented to extract bare earth and seabed reflections from the waveforms. Initial test flights of the upgraded EAARL-B system are planned in the early 2012 and the system is expected to be available as an operational-research system in March 2012.

The EAARL is a research sensor and its applications are limited to small research projects that require the unique capabilities the system and its open-source post-processing software offer. The short pulse width and low pulse energy have enabled the mapping of very shallow submerged topography in coastal and riverine environments. The upgrades to the sensor will further improve the ability to map shallow bathymetry and coastal land elevations seamlessly. The success of the EAARL sensor in coastal and riverine environments has led to a new focus in the commercial industry to develop sensors that are capable of topo-bathy mapping in the coastal zone.

CZMIL

The Coastal Zone Mapping and Imaging LiDAR (CZMIL) is a new airborne mapping and imaging system designed to simultaneously produce high resolution 3D images of the beach and shallow water seafloor, and to achieve benthic classification and water column characterization. Developed by Optech International under the auspices of the US Army Corps of Engineers (USACE) and the Joint Airborne LiDAR Bathymetry Technical Center of Expertise (JALBTCX), CZMIL is a $13 million, 5-year program to develop an integrated LiDAR-imagery sensor system and software suite designed for the highly automated generation of physical and environmental information products for mapping of the coastal zone. CZMIL is specifically designed to perform better in shallow, turbid water as compared to Optech's traditional bathymetric sensors such as the SHOALS-3000 system. To achieve this design, improvements are being made to the scanner, laser, detector, and receiver electronics. A 10 KHz laser combined with 7 segments in the segmented detector will produce a spatial resolution of 0.7 m at a nominal flying height of 400 m. The pulse width of 2.5 ns combined with improved band-width electronics and a 10-bit digitizer is expected to generate a system response function of 6 ns (compared to 20 ns for SHOALS). Coastal areas such as the surf zone and turbid waters have been especially challenging to LiDAR sensors. The improvement in the system response time is expected to achieve direct detection of the shallow seafloor in waters as shallow as 0.25 m. Further, the large aperture circular scanner provides two opportunities to penetrate the surf zone (one fore and one aft) when flying parallel to the shoreline. The CZMIL sensor is expected to be operational by early 2012 and will be deployed by the JALBTCX group for its National Coastal Mapping Program (NCMP) to provide high-resolution elevation and imagery data along U.S. shorelines on a recurring basis.

Chiroptera

Airborne Hydrography AB (AHAB) is developing a new topo-bathy system called Chiroptera intended to target the growing need for high accuracy surveys of shallow water regions. The new sensor will include two LiDAR scanners, one near-infrared scanner operating at 1064nm and one green wavelength scanner operating at 532 nm. The entire system is expected to be light-weight and deployable in a helicopter or

single-pilot airplane offering cost-efficiency during operations. The multi-sensor platform will also include a high-resolution frame camera and an optional hyper-spectral camera. The bathymetric capability is not designed to compete with the depth range of the traditional airborne bathymetric LiDARs, such as AHAB's own HawkEye II, and is expected to provide bathymetry in up to 10 m water depths. The system is expected to be made available in 2012.

Aquarius

Optech Incorporated has recently released a compact shallow-water mapping solution for its Airborne Laser Terrain Mappers (ALTM). The new ALTM Aquarius provides simultaneous terrestrial and water depth measurement capability, enabling the collection of data sets that span the entire land-water interface to depths of about 10 meters. The Aquarius is available as a sensor head addition to the ALTM Gemini product line, or a complete survey solution on its own. The current specifications for shallow water mapping includes a frequency-doubled green-wavelength (532 nm) laser with a pulse repetition rate of up to 70 KHz operating at a nominal altitude of 300-600 m AGL, enabling a 30-60 cm laser footprint on the water surface with a maximum depth penetration of about 10 m. The reflected backscatter from the ~ 6-ns-long laser pulse is captured by an Avalanche Photo Diode (APD) detector and a 12-bit dynamic-range digitizer. Initial results from a test flight conducted in Lake Ontario suggest penetration to about 12 m depths in relatively clear water. The sensor can also be operated in the "topographic mode" to capture up to 4 discrete range measurements and operated at an altitude of 300-2500 m AGL. A 12-bit waveform digitizer is optionally available for capturing waveform data.

VQ-820-G

The VQ-820-G hydrographic airborne laser scanner, being developed by Riegl, is specifically designed to survey seabeds or ground of rivers or lakes using a green-wavelength laser at 532 nm. As with the other systems described above, the VQ-820-G offers simultaneous topo-bathy acquisition at a nominal operating flight altitude of 600 m for hydrographic surveys and 2000 m for topo-only surveys. The expected measurement range is about 1 Secchi depth with a peak laser pulse rate of 250 KHz, resulting in a maximum effective measurement rate of 110,000 pulses per second. Although the system digitizes the return waveform, an online waveform processing mode creates on-the-fly discrete returns for immediate creation of a point cloud dataset. Bathymetric data processing is accomplished using Riegl's proprietary software package. Since the system is able to produce data at a very high spatial density, the water surface can be either defined as a simple plane or represented by a triangulated model acquired from the laser scan data. The scan mechanism of the VQ-820-G is based on a rotating multi-facet mirror where the scan axis is tilted by about 20˚ with respect to the nominal flight direction, so that the angle of incidence of the laser beam to the water surface varies only by about 1˚ over the entire scan range of up to 60˚. This results in an arc-like scan pattern on the ground. The beam divergence of the system is only about 1 mrad at the nominal flying altitude resulting in a tightly focused beam on the water surface.

Data Processing

Software methods and algorithms for processing LiDAR data are equally important with hardware for creating accurate topo-bathy products. Data processing techniques vary considerably from system to system, but they have a number of aspects in common such as the integration and calibration of

positioning, orientation, and laser ranging data to create a geo-referenced point cloud of LiDAR returns. In bathy LiDAR, the presence of another medium (i.e. water) along the travel path of the laser pulse requires advanced processing of the signal waveform, to account for refraction of the laser pulse at the water surface and the change in speed of light through the water column. A waveform usually includes a return from the water surface, volume backscatter from the water column and a seabed return. In turbid waters, the signal attenuates rapidly through the water column due to the absorption and scattering by organic and inorganic matter in the water column. Often, this results in a very weak seabed return. Specialized signal processing techniques are required to determine these weak seabed returns and reject the false returns from the water column. If the automated processing algorithms are unsuccessful, a manual approach is needed which is time-consuming and costly. Processing data in shallow waters requires parameterization of the transmitted and received waveform and specialized deconvolution or decomposition techniques to separate the water surface from the seabed. These enhanced software procedures for extracting reliable and accurate seabed returns in various water column conditions are currently being researched. Commercial post-processing software for topo-bathy waveform data is yet to mature into a fully- or even semi- automated process.

A few LiDAR manufacturers offer a complete hardware-software solution, which includes the automated generation of point cloud data from waveforms (such as Riegl's RiAnalyze). The Optech Rapid Environment Assessment (REA) software is image processing software that provides coastal environmental information by fusing airborne and hyperspectral data. The REA also includes a new shallow water algorithm that uses a novel signal processing approach to process shallow bathymetry using the traditional bathy LiDAR. The CZMIL Data Processing System is being developed to improve upon the REA software and provide a complete software suite for producing topo-bathy point clouds, DEMs, reflectance images, georeferenced high-resolution frame camera ortho image mosaics, classification maps, chlorophyll and CDOM concentration images, and shoreline vectors. The underlying algorithms used to process data with any of these software packages are proprietary. The airborne LiDAR processing system (ALPS) for the EAARL sensor is an open-source alternative, but the software is specifically designed to process EAARL data and needs considerable effort to customize the software for processing data from other sensors.

Applications & Challenges

We are in an exciting stage of development in bathy and topo-bathy LiDAR technology. The new commercial topo-bathy LiDAR systems are expected to provide unprecedented capabilities in mapping the coastal zone, heretofore only addressed by research systems such as the EAARL. Several current challenges in mapping submerged topography in the littoral zone will be addressed by these new systems. The increased spatial density will match those of the topographic LiDARs, thereby enabling sub-meter seamless topo-bathy data in coastal and riverine environments. The applications of these data and some of the current and future challenges are described below.

Coastal Mapping

High-resolution topography is a primary data layer for coastal management activities, and is needed for planning, navigation, development, and conservation of coastal resources. Accurate and up-to-date coastal topographic maps are required at the most basic level by land use planners to establish building

set-backs, inventory wetland and agricultural land resources, and to identify zones that are severely impacted by powerful hurricanes and storms. Many environmentally sensitive areas such as wetlands, mangroves and other coastal forests offer limited ground access due to vegetation cover and soil characteristics. These areas are easily mapped by airborne LiDAR to provide accurate and detailed representation of the horizontal and vertical structure of plant communities, as well as bare Earth topography under vegetation. In coastal areas with high population and other human and agricultural land use areas, airborne LiDAR provides a safe and reliable method to obtain topography of the terrain for disaster planning and as input for various floodplain and hydrodynamic modeling programs.

The recent developments in airborne laser ranging technology and the new systems that are being developed (described above) allow seamless topo-bathy measurements in the nearshore coastal zone. Challenges still remain in mapping in very shallow water, where the signals from the water surface and the seafloor begin to merge. The ability of a LiDAR system to measure submerged topography in this very shallow depth regime (typically 0-1 m water depth) is dictated by the laser pulse width and the overall system response time. Minimizing the footprint of the laser pulse also improves the ability to separate the water surface return from a shallow seabed return, especially in sloping terrain. All the new topo-bathy systems that are currently being developed are focusing on improved bathymetry performance in these shallow depths; the results from evaluation studies of these systems are awaited.

The surf zone remains one of the most challenging environments for laser systems to operate. A reflection from a very bright target such as foam produced by the breaking wave saturates the detector, making it blind to the entire returned laser pulse. Further, sediments and air bubbles entrained in the water column by wave breaking compromise its ability to retrieve accurate bottom elevations. Often, this limitation is mitigated with repeat data collections because there are more opportunities to cover a particular area of the beach zone when breaking waves are not present. These repeat data collections are time-consuming and cost-prohibitive. The CZMIL system is attempting to address this issue by using a new circular scanning design with the fore and aft scans in the same over flight providing two opportunities to map the same spot in the surf zone. This technique may help in eliminating returns that saturate the detector; however, within the same scan, the water clarity is unlikely to improve and the suspended sediments may still preclude the laser pulse to penetrate through to the seabed.

Aside from the system parameters that limit the operational depth range, the most significant limitation for airborne LiDAR systems is water clarity. For extremely turbid conditions, surveying may not be possible even using systems that emit very powerful laser pulses. Sometimes, it is possible to survey in deeper water and not in the shallowest water because the water is typically much clearer farther from shore. In many areas, if the water is too dirty for a survey to be successfully completed on a given day, it may be necessary to revisit that site at a different tidal phase, or several days later when the turbidity in the water has reduced to acceptable levels. The turbidity in waters is often seasonal, especially in bays and lagoons that are influenced by river outflows; hence, careful planning of surveys and knowledge of local conditions is required to produce the desired results.

Nautical Charting

Until recently, nautical charting had been the chief survey requirement for most of the airborne bathy LiDAR systems. There is an enormous backlog in the production of modern charts needed for safe navigation worldwide. A significant portion of these backlog areas are in relatively clear, shallow waters, which are well suited for bathymetric LiDAR. NOAA is responsible for providing hydrographic survey data to support safe navigation in the U.S. Exclusive Economic Zone (EEZ), which comprises 3.4 million square nautical miles and extends 200 nautical miles offshore. In the past decade, NOAA's Office of Coast Survey has contracted a series of near-shore hydrographic surveys using bathymetric LiDARs as traditional ship-based acoustic methods of surveying in waters less than 40 m are time-intensive, less complete and in very shallow waters are a dangerous undertaking for survey vessels and crew. Early projects which focused on the use of bathymetric LiDAR for nautical charting applications had met with varying degrees of success, according to a report published by the Hydrographic Society of America in 2007. The primary challenge has been the impact of environmental variability on LiDAR data. Lessons were learned from earlier studies and there is now a better understanding of the conditions that contribute to the success of a survey and determining when and where this technology may be applied.

The ability to detect underwater targets or obstructions in navigation channels is one of the fundamental requirements of hydrographic surveys. Detecting objects smaller than a 2-meter-cube has been very challenging for bathymetric LiDARs. The LiDAR point density has to be sufficiently high for detecting underwater targets with limited dimensions. The laser footprint size and field-of-view of the detector need to be large enough to illuminate and detect the object (wholly or partly), but small enough to ensure that the detected object is discernible in the return signal, and not mixed with returns from other objects or the seafloor. The new topo-bathy sensors, with their high spatial density and small footprint and receiver field-of-view, have the potential to detect underwater objects that are smaller than 1 m-cube in navigation channels. However, this may require new automated and sophisticated waveform-processing software to isolate the detected object from the water-column backscatter.

Riverine Mapping

Streams are one of the most dynamic components of landscapes, and their modern morphology represents not only a response to contemporary sediment and water supplies, but also reflects a legacy of past environmental conditions. Cost and logistics typically limit detailed stream studies to small spatial extents, making it difficult to analyze interactions among larger channel domains or to extrapolate to the scale of stream networks. Further, management of aquatic habitat in streams requires description of conditions and processes both inside the channels and in the adjacent riparian zones. The need for detailed channel topography is often driven by the recent development of physical and biological models that have provided unprecedented predictive capabilities. Simulation of floodplain flows using two-dimensional models and the complex velocity and flow models used in habitat studies require very detailed and accurate topography of the channel bed and surrounding floodplain. The first generation EAARL system has been used in several studies to assess channel and floodplain conditions in rivers in the Northwest. An EAARL survey of the upper Bear Valley Creek in Idaho was successful in mapping many long reaches of pool-riffle bathymetry and the topography of the surrounding floodplain

(Figure G.23). The new breed of commercial topo-bathy sensors is expected to provide the high-resolution, continuous sub-aerial and sub-aqueous topography data that support integrated analyses of channel, floodplain, and riparian ecosystems at scales spanning short reaches to whole stream networks.

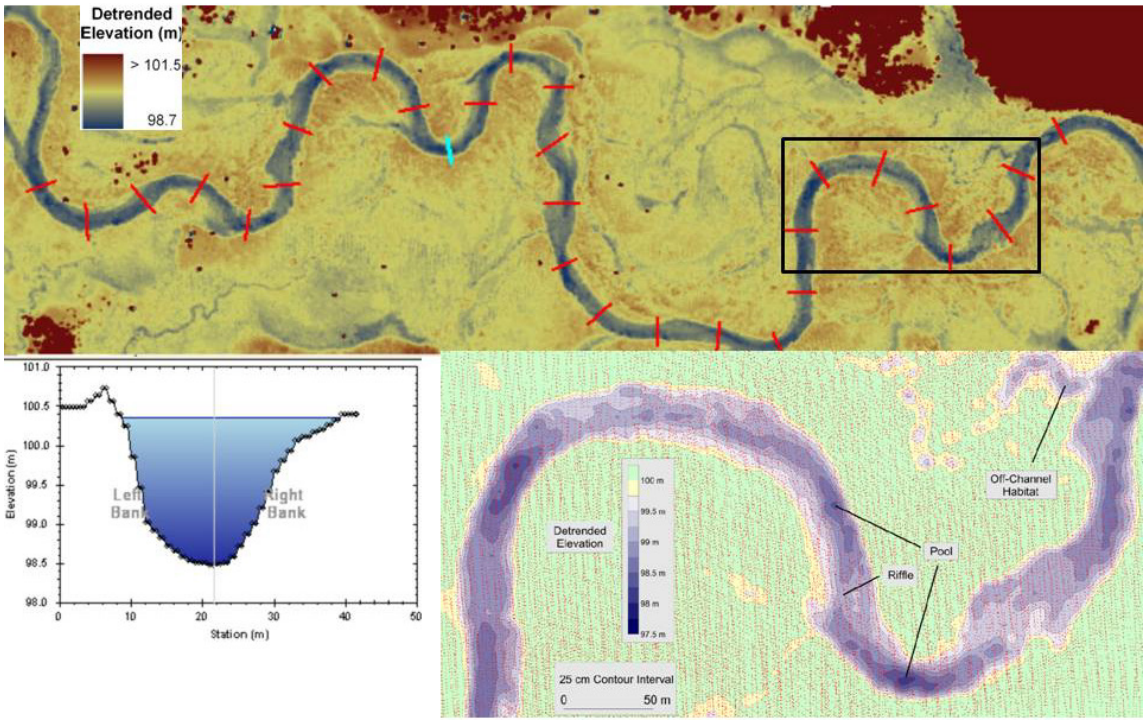

Figure G.23. Topo-bathy DEM of lower Bear Valley Creek, Idaho, USA, acquired by the EAARL sensor in 2007 (*top*). The river flows left to right. The elevations are "detrended" to remove the general channel gradient which obscures other significant topographic features, such as pools and riffles. The red lines across the river are cross sections spaced at 100 m intervals. *Lower Right:* A detailed bathymetric contour of a section of this reach (image extent is the rectangular box outlined in the top image). The red dots illustrate the density of data from multiple passes made by the LiDAR sensor. *Lower left:* A cross section (location shown as a blue line across the river in the top image) depicting the channel hydraulic geometry and estimated water level [Source: McKean et al, 2009].

Data Fusion

In recent years, there has been an increasing demand for collection and fusion of topography and imagery in terrestrial and bathymetric environments to enable classification of habitats. The acquisition of high-resolution LiDAR data along with multi- and hyper-spectral imagery presents several operating constraints. The various data collection requirements for each technology create a very small window of opportunity to complete the survey. For example, sun angle can play a significant role in defining the timing for a multispectral survey; however, LiDAR surveys are generally not affected by sun angle and are often flown during night time. Nevertheless, fusion of LiDAR and imagery can give additional information relevant to environmental studies such as seafloor classification, and hydrographic requirements such as target detection. The CZMIL sensor and the Data Processing System, described above, are being developed as a complete mapping and imaging solution to create high-resolution 3D seafloor imagery and reflectance maps along with several parameters that describe the water column (Figure G.24).

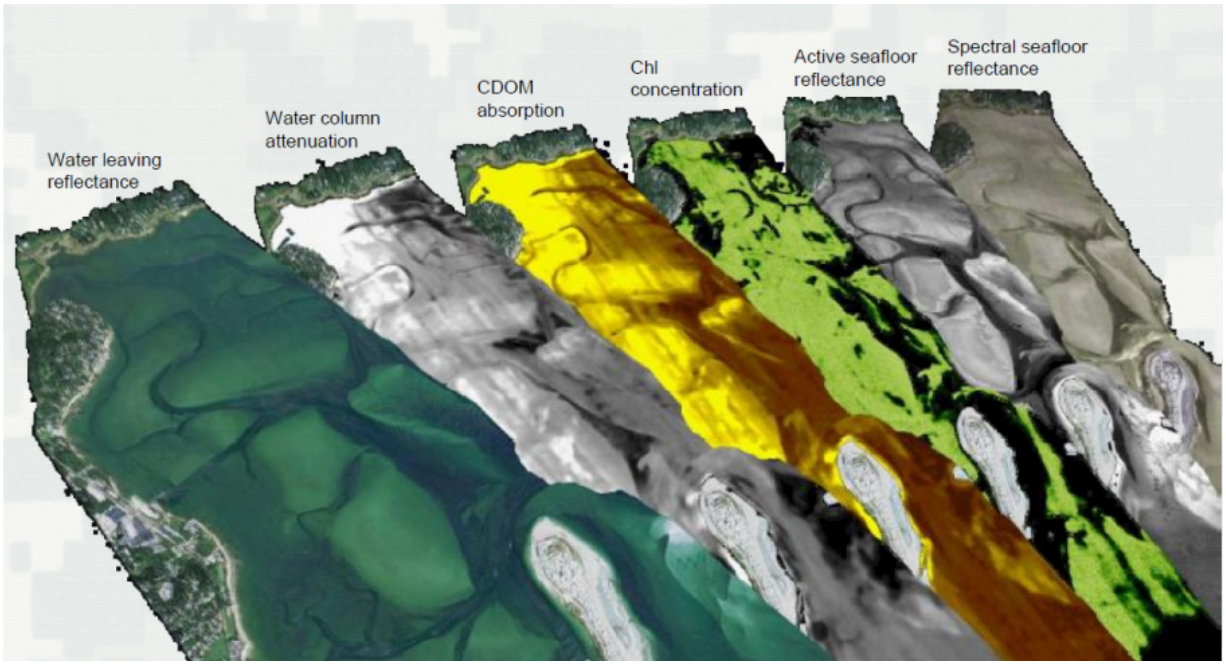

Figure G.24. Example products expected to be derived from the CZMIL sensor using the new Data Processing System being developed by Optech [Image courtesy: Christopher Macon, USACE].

Bathymetric LiDAR Technology Conclusions

- As with topographic LiDAR, technology trends show continued evolutionary improvements in topobathymetric LiDAR system technologies.
- For coastal mapping starting in 2012, JALBTCX is expected to employ multiple CZMIL systems to start collecting topobathymetric data of U.S. coastlines for the National Coastal Mapping Program.
- For nautical charting, NOAA's Office of Coast Survey will be better able to perform its mission with emerging bathymetric LiDAR systems that perform better in turbid and/or shallow waters.
- For riverine mapping, many federal and state agencies are eager to see if emerging topobathymetric LiDAR systems will in fact be able to map rivers and streams that are turbid and/or shallow; this is the major need currently unmet by today's topobathymetric technologies.

Bathymetric LiDAR Image References

Figure G.20: Guenther, G.C., 2007: Digital Elevation Model Technologies and Applications: The DEM Users Manual, 2nd Edition, D. Maune, ed., American Society for Photogrammetry and Remote Sensing, Chapter 8: Airborne LiDAR bathymetry, 253-320.

Figure G.21: Nayegandhi, A., Wright, C.W., Brock, J.C., 2009,EAARL: An Airborne LiDAR System for Mapping Coastal and Riverine Environments, in Bayer, J.M., and Schei, J.L., eds., PNAMP Special

Publication: Remote Sensing Applications for Aquatic Resource Monitoring, Pacific Northwest Aquatic Monitoring Partnership, Cook, Washington, chap. 1, p. 3-5.

Figure G.22: Nayegandhi, A., Brock, J.C., 2008,Assessment of Coastal Vegetation Habitats using LiDAR. In: Yang X. (ed) "Lecture Notes in Geoinformation and Cartography - Remote Sensing and Geospatial Technologies for Coastal Ecosystem Assessment and Management": Springer Publication pp 365-389

Figure G.23: McKean, J.; Nagel, D.; Tonina, D.; Bailey, P.; Wright, C.W.; Bohn, C.; Nayegandhi, A. Remote Sensing of Channels and Riparian Zones with a Narrow-Beam Aquatic-Terrestrial LIDAR.*Remote Sens.*2009,*1*, 1065-1096.

Risk Factors

Identify key risks that could hamper a consistent national implementation such as geoid errors, lack of developed or accepted national guidelines/standards for data collection and handling, the need for better QA/QC procedures for LiDAR systems and derived data (which impact accuracy and data consistency across projects), the maturity of software for extracting information from discrete return and waveform data, industry capacity to perform national scale collection, etc. The Contractor shall identify the key technical limitations and provide an estimate of the resources needed to address these limitations.

Potential Changes to Horizontal and Vertical Datums

A *geodetic datum* is a set of constants specifying the coordinate system used for geodetic control, i.e., for calculating the coordinates of points on the Earth. A geodetic datum essentially defines the origin and orientation of horizontal and vertical coordinate systems, where the origin identifies the location of "zero" in measuring longitude, latitude, and elevation relative to the origin.

A *horizontal datum* is a geodetic datum that specifies the coordinate system in which horizontal control points are located. The North American Datum of 1983 (NAD 83) is the official horizontal datum in the U.S. Since the establishment of NAD 83, the National Geodetic Survey (NGS), in cooperation with other federal, state and local surveying agencies, conducted a resurvey of the U.S. using GPS observations often referred to as the High Accuracy Reference Networks (HARNs) and since 1994 has implemented a network of GPS Continuously Operating Reference Stations (CORS). Continued improvements in GPS technology and requirements from users of spatial data will eventually require a transition to an improved global reference frame based on the International Terrestrial Reference Frame (ITRF) which accounts for movements between continents. NGS already publishes ITRF coordinates for all CORS in the U.S. NGS will continue to maintain and improve NAD 83 as the official horizontal datum of the U.S. until such time as it no longer supports requirements for surveying, mapping and navigation. In the meantime, NGS provides the Horizontal Time Dependent Positioning (HTDP) software that enables users to estimate horizontal displacement and/or horizontal velocities related to crustal motion in the U.S. and its territories. The software enables users to update positional coordinates and/or geodetic observations to a user-specified date. NGS has proposed a new geometric horizontal datum – the National Spatial Reference System (NSRS) to replace NAD83 by 2018. The NSRS will be accurately tied to the International Terrestrial Reference Frame (ITRF) and accessible to GNSS users anywhere in the United States and its territories. For all practical purposes, an ITRF based geodetic datum and the World Geodetic System of 1984 (WGS84), the reference system for GPS, are the same; the difference is on the order of a few centimeters.

A *vertical datum* is a set of constants that define a height (elevation) system. It is defined by a set of constants, a coordinate system, and points that have been consistently determined by observations, corrections and computations. The North American Vertical Datum of 1988 (NAVD 88) is the official vertical datum in the conterminous U.S. island areas (e.g., Hawaii, American Samoa, Puerto Rico, etc.) have their own local vertical datum. There are three fundamentally different types of vertical datums –

ellipsoid, orthometric, and tidal. Figures G.25 and G.26 show the relationship between ellipsoid heights, orthometric heights and geoid heights.

- Ellipsoid heights (h) are referenced to a mathematically-defined reference ellipsoid. The ellipsoid height of a point on the Earth's surface is the distance from the reference ellipsoid to the point, measured along the line which is normal (perpendicular) to the ellipsoid. All heights from GPS surveys (ground or airborne) provide heights above the smooth, mathematical ellipsoid. Ellipsoid heights follow rules of geometry.

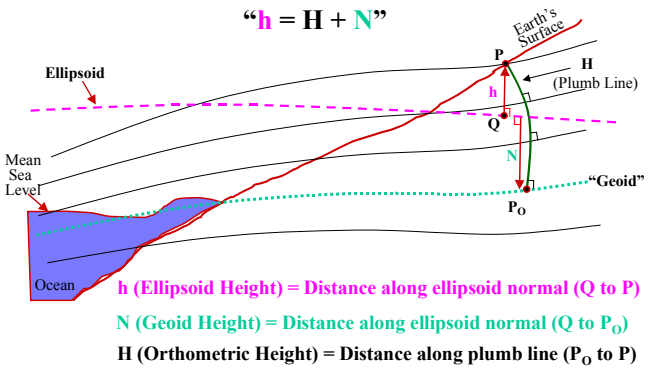

Figure G.25. Relationships between ellipsoid, geoid, and orthometric heights.

- Orthometric heights (H) are referenced to a gravimetrically-defined equipotential reference surface, the geoid, which undulates with changes in gravity throughout the Earth. The orthometric height of a point on the Earth's surface is the distance from the geoidal reference surface to the point, measured along the plumb line normal to the geoid. Orthometric heights, more commonly known as "elevations," follow rules of gravity. Because the flow of water follows the rules of gravity, all references to "elevations" in this report equate to orthometric heights.
- Geoid heights (N) are the difference between ellipsoid heights and orthometric heights for the same points on the Earth's surface, i.e., N = h – H. This is the same as H = h – N when computing orthometric heights from ellipsoid heights obtained from photogrammetry, LiDAR or IFSAR.

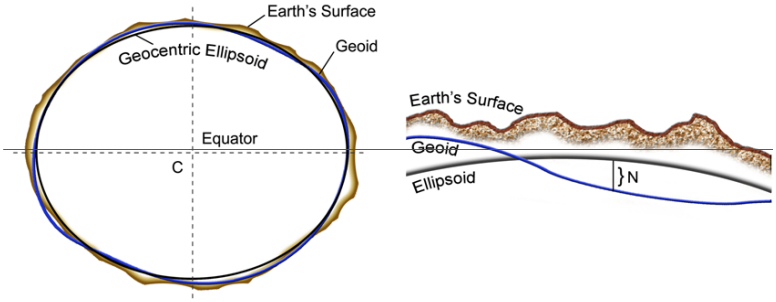

Figure G.26. Relationship of the Earth's surface, the geoid and a geocentric ellipsoid. The height difference between the geoid and the ellipsoid is the geoid separation. [Image from URS Corp.]

The geoid is the equipotential surface of the Earth's gravity field which best fits, in a least squares sense, global mean sea level. The geoid is theoretical only. You can't see it, touch it or even dig down to find it. Simply put, the geoid is the natural extension of the mean sea level surface under the landmass. For example, if we dug an imaginary trench across the country linking the Atlantic and Pacific oceans, and if we allowed the trench to fill with seawater, the surface of the water in the trench would represent the

geoid. Although theoretical, the geoid remains the basis for determining elevations in Kansas, for example, though over a thousand miles away from the nearest ocean.

NGS has a federal mandate to provide accurate positioning, including heights, to all federal non-military mapping activities in the U.S. In 2007, NGS embarked on the GRAV-D Project (Gravity for the Redefinition of the American Vertical Datum). This undertaking was driven by the fundamental connection between the Earth's gravity field and the very definitions of "heights" or "elevations." Accurate gravity data are the foundation for the government's determinations of heights and elevations.

In the past 20 years, the use of GPS technology for determining fast and accurate *ellipsoid heights* has created a pressing need for a similarly fast and accurate determination of *orthometric heights*. *Ellipsoid heights* (from photogrammetry, LiDAR or IFSAR) cannot be used to determine where water will flow, and therefore are not used in topographic/floodplain mapping. *Orthometric heights* are related to water flow and are most useful for all forms of elevation mapping. In order to transform from *ellipsoid heights* to *orthometric heights* (elevations), a model of the geoid must be computed, and geoid modeling can only be done with measurements of the acceleration of gravity near the Earth's surface. GRAV-D is NGS' initiative to redefine the vertical datum of the U.S. by 2021. The gravity-based vertical datum resulting from this project will be accurate at the 2 cm level for much of the country. The project is currently underway and actively collecting gravity data across the U.S. and its territories. As shown previously in Figure G.5, changes in orthometric heights (elevations) will vary from zero in Florida to over 1 meter in Washington and approximately 1.5 meters (4.9 feet) in the North Slope Borough of Alaska. Changes in the new vertical datum, projected for 2021 or 2022, will impact all elevations in the NED. There are at least three ways to convert elevations from prior vertical datums to the new vertical datum:

1. For new acquisitions of elevation data, retain all ellipsoid heights (as well as orthometric heights) so that the new geoid heights can be applied to the original ellipsoid heights in the 2020s for computation of new orthometric heights relative to the new vertical datum. This option approximately doubles the storage requirement for maintenance of orthometric heights as well as ellipsoid heights during the coming decade.
2. For existing elevation data, ensure that the metadata includes the geoid model used to convert ellipsoid heights to orthometric heights. Then, when the new vertical datum is adopted, reprocess all existing orthometric heights to remove the old geoid heights and add the new geoid heights to the formula $H = h - N$
3. For existing elevation data, ensure that the metadata includes the geoid model used to convert ellipsoid heights to orthometric heights. For each old geoid model (e.g., Geoid99, Geoid03, Geoid09, etc.) develop geoid height difference models (ΔN) that apply corrections to the old orthometric heights to convert them to new orthometric heights (elevation) referenced to the new vertical datum.

Capacity, Timeliness, Costs of LiDAR Acquisitions

Capacity: In addition to LiDAR sensors at government agencies including military and university-owned, there are approximately 60 commercial wide-area LiDAR sensors now in operation in the U.S. and Canada with pulse repetition rates between 100 kHz and 500 kHz. Most are discrete-return systems but

some are full-waveform sensors and many could have external waveform options added if required. Additional sensors are expected to be acquired in the years ahead.

In estimating the capacity of average LiDAR sensors, Dewberry made the following assumptions, based on input from USGS' multiple GPSC2 contractors:

- 160 acquisition days/sensor per leaf-off season, recognizing that numbers vary geographically between a low of 60 days/year in the (rainy/foggy) Pacific northwest, to 120 days/year in the north where snow is a factor, to 200+ days/year in the south where snow is not a factor
- 4 hours/day available on average for acquisition when considering delays for weather and aircraft maintenance
- 20 km^2/hour when acquiring QL1 LiDAR with 8 points/m^2 in flat terrain; 15 km^2/hour with terrain; average 17.5 km^2/hour (11,200 km2/year/sensor)
- 60 km^2/hour when acquiring QL2 LiDAR with 2 points/m^2 in flat terrain; 45 km^2/hour with terrain; average 52.5 km^2/hour (33,600 km^2/year/sensor)
- 85 km^2/hour when acquiring QL3 LiDAR with 1 point/m^2 in flat terrain; 65 km^2/hour with terrain; average 75 km^2/hour (48,000 km^2/year/sensor)

For the lower 48 states (3,008,354 square miles or 7,791,601 square kilometers), Table G.5 estimates the number of LiDAR sensors required if LiDAR is acquired for the five update frequencies indicated. Assuming the availability of 60-70 sensors by 2014, green indicates minimal risk of failure in meeting acquisition goals; yellow indicates moderate risk of failure in meeting acquisition goals; and red indicates high to very high risk of failure in meeting acquisition goals. This table does not account for LiDAR acquisition for Hawaii, Puerto Rico, Virgin Islands, American Samoa, Guam or the Northern Marianas Islands which are evaluated separately.

Table G.5. Estimated Number of LiDAR Sensors Required for Different Quality Levels and Update Frequencies

Update Frequency	If QL1 LiDAR Collected at a rate of 17.5 km^2/hour	If QL2 LiDAR Collected at a rate of 52.5 km^2/hour	If QL3 LiDAR Collected at a rate of 75 km^2/hour
Annually	697	232	162
2-3 years (average 2.5 years)	279	93	65
4-5 years (average 4.5 years)	155	52	36
6-10 year (average 8 years)	87	29	20
>10 years (average 15 years)	46	15	11

Timeliness: From a timeliness perspective, the risks are somewhat higher because some of the small acquisition firms acquire LiDAR data only and do not perform their own post processing. This would increase demands upon those firms that do perform LiDAR post processing to ensure data satisfies requirements of USGS v.13 or other standards for QL1 or QL2 LiDAR to be developed.

Costs: From a cost perspective, the risks are minor for the 48 conterminous states because advancements in hardware and software are expected to cause unit pricing to decrease. However, the costs/km^2 is much higher for Hawaii and island territories because of logistical issues; these islands require a different cost model which could be doubled for Hawaii and much higher still for American

Samoa, Guam and the Northern Marianas Islands where airborne LiDAR may not be feasible at all. Puerto Rico and the U.S. Virgin Islands will cost more per square kilometer than in the 48 conterminous states, but not as much as Hawaii which is farther away from the mainland.

Standards and Guidelines

The draft "USGS Lidar Guidelines and Base Specification," Version 13 (v.13), is currently the *de facto* industry standard for delivery of Quality Level 3 LiDAR data as defined for the National Enhanced Elevation Assessment. Under V.13, deliverables include metadata, raw point cloud, classified point cloud, bare earth surface (raster DEM), and breaklines used in hydro-flattening. Most LiDAR data acquired by USGS and FEMA during the past two years have been produced to v.13 standards. V.13 is expected to undergo very minor changes before it is finalized as USGS' national standard for acquisition and delivery of Quality Level 3 LiDAR products.

- For the Collection Phase, v.13 specifies requirements for discrete returns as well as waveform data to include: intensity values; nominal pulse spacing (NPS); data voids; spatial distribution; scan angle; absolute vertical accuracy; relative accuracy; flightline overlap; collection area buffers; and collection conditions.
- For Data Processing and Handling, v.13 specifies LAS classes 1, 2, 7, 9, 10 and 11; GPS times; horizontal and vertical datums; Coordinate Reference System; units of measure; swath file sizes and File Source IDs; point families; raw data deliverables; positional accuracy validation; classification accuracy; classification consistency; and tiling scheme.
- For Hydro-Flattening, v.13 specifies hydro-flattening procedures for inland ponds and lakes; dual-line inland streams and rivers; non-tidal boundary waters; tidal waters; breaklines; and optional single-line streams.
- For Deliverables, v.13 specifies requirements for metadata; raw point cloud; classified point cloud; bare-Earth DEM (raster); and breaklines.
- For Common Data Upgrades, v.13 specifies optional independent 3rd party QA/QC by another AE Contractor (encouraged); higher NPS (point density); increased vertical accuracy; full waveform collection and delivery; additional environmental constraints (tidal coordination and shorelines corrected for tidal variations); top-of-canopy digital surface model (DSM); intensity images; detailed LAS classification (additional classes 3, 4, 5, 6, n); hydro-enforced and/or hydro-conditioned DEMs; breaklines for single-line hydrographic features; breaklines for other features to be determined; extracted building footprints; and other products to be negotiated.

Whereas v.13 serves as USGS' Lidar Guidelines and Base Specification for Quality Level 3 LiDAR, it could easily be changed to serve as USGS' Lidar Guidelines and Base Specifications for LiDAR Quality Levels 1 and 2 as well. Only the absolute vertical accuracy and nominal pulse spacing (NPS) would need to change to accommodate QL1 and QL2 requirements.

For QL5 IFSAR data, Intermap's *Product Handbook and Quick Start Guide* serves as the IFSAR guidelines and specifications for NEXTMap® USA data available nationwide except for Alaska and for any future airborne IFSAR acquisition projects.

Whereas future elevation datasets can be produced to any of the five established Quality Levels (QLs), existing elevation datasets do not necessarily coincide with any of these QLs. To avoid risks of overstating the quality of existing elevation datasets produced to different standards, the following guidelines are provided:

- If a LiDAR dataset satisfies 1-foot vertical accuracy requirements in open terrain (RMSEz ≤9.25 cm) but has point density somewhere between 2 and 8 points per square meter, it is considered the equivalent of QL2, having less than 8 points per square meter required for QL1. Used to compute point density, the Nominal Pulse Spacing (NPS) assessment is made against single swath, first return data located within the geometrically usable center portion (typically ~90%) of each swath.
- If a LiDAR dataset has RMSEz somewhere between 9.25 cm and 18.5 cm in open terrain, it is considered the equivalent of QL3, having RMSEz of 18.5 cm or better. (Data produced to the USGS V13 standard fits in this category, with RMSEz of 12.5 cm in open terrain.)
- If a LiDAR dataset has RMSEz ≤18.5 cm in open terrain, but >18.5 cm in vegetation and/or other land cover categories, it is considered equivalent to QL3 if the Consolidated Vertical Accuracy (CVA) is ≤36.3 cm; but if the CVA is >36.3 cm, it is considered equivalent to QL4.
- If a LiDAR dataset has RMSEz >18.5 cm in open terrain and/or >2 meter Nominal Pulse Spacing, it is considered equivalent to QL4.
- DEMs produced from stereo imagery are not necessarily QL4. For example, if the flying height and geometry supports the production of photogrammetric contours with 2-foot contour accuracy (RMSEz ≤18.5 cm) or better, and with DEM post spacing ≤2 meters, DEMs produced from such imagery is considered equivalent to QL3.
- All IFSAR DEMs produced from existing NEXTMap® USA or new IFSAR data acquisition programs are assumed to satisfy QL5 requirements.

The "USGS Lidar Guidelines and Base Specification," Version 13 (v.13), only pertains to topographic LiDAR point cloud data, hydro-flattened gridded DEMs, and breaklines used for hydro-flattening. If USGS also provides DEMs that are hydro-enforced or have no hydro processing, of if USGS provides DSMs, contours, hillshades, slope maps, aspect maps, curvature maps, or additional breaklines, for example, each of these products would also require guidelines and specifications so that users would know what to expect from such enhanced elevation derivative products.

QA/QC Procedures

Released in 1998, the National Standard for Spatial Data Accuracy (NSSDA) provides a methodology for testing and reporting the absolute accuracy of geospatial data, but the NSSDA provides no accuracy thresholds for different levels of accuracy and as such is not a true standard. In its 2004 "Guidelines for Digital Elevation Data," the National Digital Elevation Program (NDEP) provided procedures for testing the Fundamental Vertical Accuracy (FVA), Supplemental Vertical Accuracy (SVA) and Consolidated Vertical Accuracy (CVA) of LiDAR data; and the American Society for Photogrammetry and Remote Sensing (ASPRS), in its 2004 "ASPRS Guidelines: Vertical Accuracy Reporting for Lidar Data," adopted the FVA, SVA and CVA methodology and linked RMSEz values to "equivalent contour intervals." None of these guidelines establish accuracy thresholds.

The Federal Emergency Management Agency (FEMA), in its "Procedure Memorandum No. 61 – Standards for Lidar and Other High Quality Digital Topography," released in 2010, aligned its requirements to the USGS "Lidar Guidelines and Base Specification v.13," with minor variations, while accepting the NDEP and ASPRS procedures for testing the FVA, SVA and CVA. For areas of 2,000 square miles or less, FEMA specifies a methodology for testing the vertical accuracy of LiDAR, requiring a minimum of 60 QA/QC checkpoints, i.e., 20 QA/QC checkpoints as a minimum in open terrain for computation of the FVA, as well as 20 QA/QC checkpoints each for two other land cover categories representative of flood plains to be mapped for computation of CVA and SVAs. When testing LiDAR data for suitability for flood hazard mapping, FEMA's requirements have become the LiDAR industry's *de facto* standard for testing the vertical accuracy of LiDAR in different land cover categories. For other applications, the USGS v.13 specifies FVA, SVA and CVA requirements without dictating the minimum number of QA/QC checkpoints to be used in different land cover categories. Procedures for testing the FVA, SVA and CVA are now mature and well understood by those who routinely deliver LiDAR products to USGS and/or FEMA.

For absolute accuracy testing of LiDAR data for 1-degree cells (between 3,000 and 4,000 square miles each), a minimum of 120 QA/QC checkpoints should be surveyed in the interior of each cell for consistency with FEMA requirements -- 40 each in three major land cover categories, and including at least 20% of the checkpoints in each quadrant of each 1-degree cell. Additionally, Dewberry recommends eight QA/QC checkpoints in open terrain along each 1-degree boundary of meridians and parallels, and within 100 meters of these 1-degree meridians and parallels, for ease in edge-matching when adjoining cells are produced by different firms. LiDAR for all cells should be acquired with a minimum of 200 meter over-edge so that cells on both sides of the 1-degree meridians and parallels can be tested by the checkpoints along those boundaries and so that there is some overlap between data from adjoining vendors. On average, this amounts to 136 QA/QC checkpoints per 1-degree cell and is considered part of the cost of nationwide LiDAR.

In addition to absolute accuracy testing, the USGS v.13 guidelines specify "Relative accuracy ≤7cm RMSEz within individual swaths; ≤10cm RMSEz within swath overlap between adjacent swaths." Whereas GeoCue and other software packages automate this testing for relative accuracy, the relative accuracy testing process remains controversial, especially by those who favor small swath overlap (e.g., 10%) compared with those that favor large swath overlap (e.g., 50%). The USGS v.13 guidelines also specifies criteria for Classification Accuracy and Classification Consistency, e.g.,: "Within any 1km x 1km area, no more than 2% of non-withheld points will possess a demonstrably erroneous classification value."

If LiDAR datasets do not undergo rigorous QA/QC accuracy testing and qualitative assessments, risks are high that adjoining datasets will not fit together seamlessly when joined. Even if the spatial accuracy of datasets is high and rigorous QA/QC has been done on both, adjoining datasets may still not fit together seamlessly. For example, if the datasets were acquired at different times of year (or in different years), there could be discontinuities due to actual changes in elevation (e.g., seasonal changes, subsidence, etc.) Furthermore, even if the vertical uncertainty (expressed in terms of RMSE) of each of the adjoining datasets is only 5 cm, there could still be a 10 cm step at their intersection. Dewberry has tested

numerous countywide datasets (all tested to 2-foot contour accuracy or better) with edge-join errors of two feet or more along county boundaries. This would be unacceptable for inclusion in the NED. All QA/QC checkpoints should be surveyed in conformance with NOAA Technical Memorandum NOS NGS-58, *Guidelines for Establishing GPS-derived Ellipsoid Heights (Standards: 2 cm and 5 cm)* or equivalent procedures that ensure that QA/QC checkpoints are at least three times more accurate, relative to the CORS network, than the elevation datasets to be tested.

Derivative Products

In addition to raw point cloud and classified point cloud data (341 requests), the standard products delivered to USGS per USGS v.13 includes the bare-earth raster DEM and breaklines used for hydro-flattening. If LiDAR full waveform data are provided to USGS (106 requests), this too could potentially be provided by USGS though users would require specialized software to use it. The remaining elevation products and derivatives requested are discussed below. The numbers of requests, shown below in parentheses, indicate the number of responses received from the on-line questionnaire asking users to identify elevation products and derivatives that they require and use.

DTM and/or DSM

- Digital Terrain Model (DTM) (413 requests): The DEM and breaklines provided by USGS V.13 comprise a DTM. Whereas both map the bare-earth terrain, the major difference between a DEM and DTM is that the DEM has a uniform grid whereas the DTM can include irregularly-spaced mass points and breaklines. DEMs and limited breaklines are currently provided by the NED.
- Digital Surface Model (DSM) (253 requests): Not currently provided by USGS. The first returns from LiDAR point cloud data yield the DSM; users can generate their own DSMs if they have standard GIS software. IFSAR data also yield DSMs. DSMs could be provided to the public if USGS had the resources to do so.

Hydrologic Processing

- Hydro-Enforced DEMs (295 requests): Not currently provided by USGS. Used for many forms of hydrographic and hydraulic modeling, this is more popular than the hydro-flattened DEMs produced by USGS for mapping applications. Most hydro-enforcement is performed by engineers who apply their own rules for hydro-enforcement. Hydro-enforcement can become very expensive, especially when including all small culverts that drain water from one side of the road to the other. Figure G.27 shows how water is erroneously diverted along the road until it intersects the water channel near the bridge, whereas G.28 shows how a breakline is used to "cut" the probable culvert beneath the road. Whereas this example is logical, not all culverts are so logical, and some culverts enable water to flow in either direction. Hydro-enforced DEMs could be potentially provided to the public.
- DEM with no Hydro Processing (255 requests): This is more popular than the hydro-flattened DEMs produced by USGS for mapping applications, but differences are minor. DEMs with no hydrographic processing could potentially be provided to the public.
- Hydro-Flattened DEM (236 requests). This is a standard deliverable per USGS v.13.

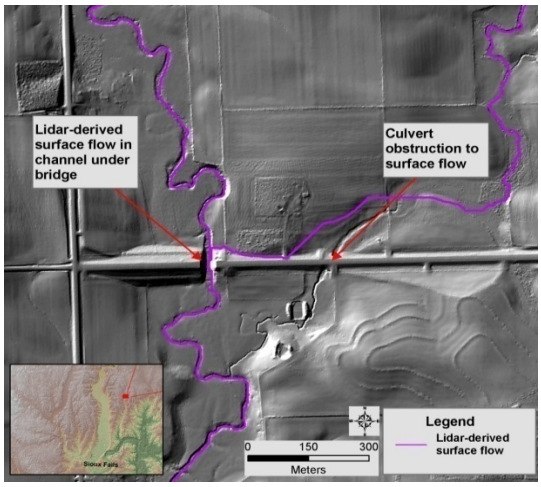

Figure G.27. Without hydro-enforcement, H&H models erroneously depict the flow of water.

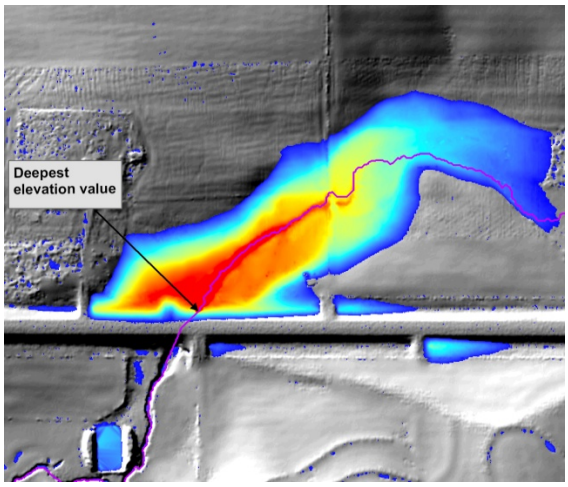

Figure G.28. With hydro-enforcement, culverts are "cut" through the DEM to model expected water flow.

Contours and/or Hillshades

- Contours (391 requests): Whereas irregularly-spaced DTMs or gridded DEMs are used for computerized analyses of bare-earth terrain surfaces, contours have long been used for human visualization of terrain surfaces. It requires time and expense to make the contours aesthetically pleasing, especially for treatment of roads and drainage features as shown in Figure G.29. With standard GIS software, users can generate their own contour lines, but they are normally noisy and not aesthetically pleasing. The recommended alternative is to use hillshades which are simple to produce.
- Hillshades (307 requests): Not currently provided by USGS. Users with their own GIS software can generate their own hillshades; however, this is an application that is ripe for commercial development as user applications on personal computers and smart phones. See Figure G.30. Figures G-29 and G-30 are not of the same area but show two forms of visual 3-D representation.

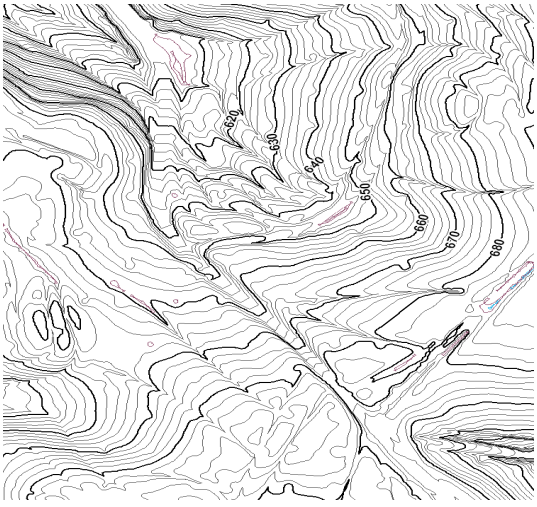

Figure G-29. Used for human visualization, contours require extensive and expensive manual editing to make them aesthetically pleasing and smooth.

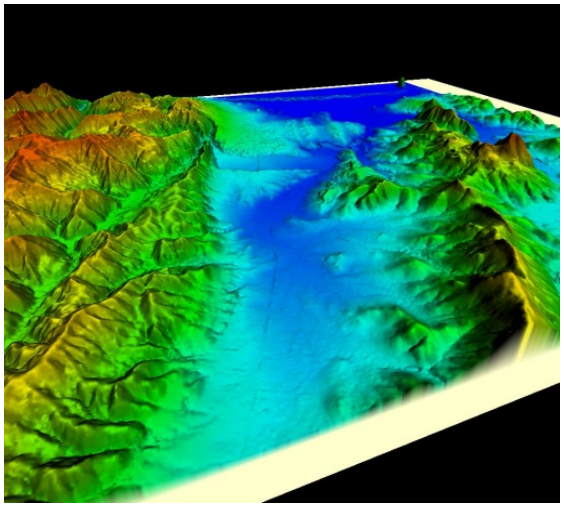

Figure G-30. Also used for visualization, hillshades require no manual editing but simple designation of sun angle and azimuth for choice of perspective view.

Slope, Aspect and/or Curvature

- Slope Data (324 requests): USGS currently provides slope data via EDNA (Elevation Derivatives for National Applications) for 1-arc-second data only. Users with their own GIS software can generate their own slope maps using higher-resolution DEMs or point cloud data.
- Aspect Data (252 requests): USGS also currently provides aspect data via EDNA for 1-arc-second data only. Users with their own GIS software can generate their own aspect maps using higher-resolution DEMs or point cloud data.
- Curvature Data (131 requests). USGS currently does not provide curvature data via EDNA (Elevation Derivatives for National Applications). Instead, curvature data are user-generated using standard GIS software.

Slope, aspect and/or curvature maps could be provided to the public if USGS had the resources to do so.

Impractical Elevation Derivative Products

- Triangulated Irregular Networks (TINs) (259 requests): Although TINs are often used to create other products (e.g., gridded DEMs, contours, slope maps), it is not realistic for TINs to be provided to the public because TIN triangles cross tile boundaries and are not easily tiled for distribution, and because TINs have much larger file sizes, carrying the topological data structure of each individual TIN triangle relative to adjoining triangles. TINs can best be produced by users with their own GIS software.
- Breaklines (256 requests): USGS collects breaklines only as required for hydro-flattening. Breaklines can be very expensive to compile, but there is a decreased need for breaklines as there is an increase in LiDAR point density. Because there are many different types of breaklines, this task is best left to individual users who best know their requirements for breaklines and best know what they can afford.
- Cross Sections (239 requests): USGS does not provide cross sections and it is unrealistic for USGS to do so in the future because there are an infinite number of possible cross sections that could be drawn within each cell of LiDAR data. Users with GIS software must generate their own cross sections to meet their unique needs.

Data Lifecycle Management and Maintenance

OMB Circular A-16, "Coordination of Geographic Information and Related Spatial Data Activities," designates USGS as the lead Agency for terrestrial elevation data. Elevation data constitute a key base layer of *The National Map*. In order for any of the layers of The National Spatial Data Infrastructure (NSDI) Framework to conform to and fit the earth surface, elevation data must be applied. Geospatial data are generally presented (viewed on a screen or printed on paper) as a two-dimensional representation of features on the earth's surface. In order for the two-dimensional presentation to be an accurate representation of these real features, their relative position must be adjusted to fit the three-dimensional surface of the earth. Elevation data are used to rectify the two-dimensional geospatial data to ensure an accurate and realistic presentation in two dimensions.

USGS has developed a multi-tiered strategy for coordination of elevation activities. USGS has supported the NSDI Framework model for elevation data and has enabled access to national coverages of Framework elevation data. Collection of the data has been executed primarily through joint planning and partnerships with others. Recognizing that many other organizations are involved in collection of elevation data, USGS has led in the development of the National Digital Elevation Program (NDEP) to provide a vehicle for standardization and coordination of elevation activities throughout the national geospatial data community. The NDEP charter includes the cooperative collection of data acquisition plans for all the member agencies and a commitment to use the cumulative plans to enable partnerships for collection of elevation data and reduce redundant or duplicative collection of elevation data. A high level of commitment exists among the membership to make these elevation assets available in the public domain, to maximize the value of the investments.

Potential Benefits

The most conservative dollar benefits were used for the Benefit Cost Analysis, versus the potential benefits. For many Business Uses, the potential benefits listed in Appendix E are believed to be more realistic than the conservative benefits, for five major reasons:

1. Of the 67 Federal Functional Activities, nearly half listed major time/cost benefits but were unable to estimate dollar savings for the government or the public.
2. Of the 329 state Functional Activities, less than half were able to estimate dollar savings to the government or the public, even though they listed major time/cost benefits.
3. Only a very small percentage of county, regional, city/town or tribal governments were interviewed for this assessment. A full accounting or extrapolated projection of all local government benefits might be several orders of magnitude greater than what was discovered in this assessment. No regional, city/town or tribal government benefits were included in the Benefit Cost Analysis because shapefiles were not provided for use in the master geodatabase used for the B-C analysis and the local government sample size could not support national projections.
4. The conservatively-estimated dollar benefits of LiDAR for Land Navigation and Safety was only $316,000/year whereas the potential benefits are over $7 billion/year. This major difference is largely caused by two factors:
    a. State Departments of Transportation rarely enjoy the benefits of statewide LiDAR and do not yet realize that wide-area LiDAR costs much less per square mile than they currently pay per linear mile for selected transportation corridors mapped by alternative means. With nationwide LiDAR, many routine topographic survey requirements will be solved for all roads, and not just for selected routes.
    b. Intelligent Transportation System (ITS) and Advanced Driver Assistance System (ADAS) technologies, based on LiDAR-derived 3-D road geometry, have not yet been implemented in new cars, trucks and busses. Expected to save at least 4% in fuel consumption starting in 2014, annual benefits to the public has the potential to save Americans tens of billions of dollars annually.
5. The total conservatively-estimated benefits are about $1.4 billion/year whereas the potential benefits are approximately $13.3 billion/year.

Risk Factor Conclusions

- The change to the new vertical (geopotential) reference frame will be a combination of the geoid model developed primarily through GRAV-D and the adoption of the geometric reference frame aligned to ITRF. Consequently, all elevations will be a function of geoid refinements and are expected to change. This will cause all elevation values computed this decade to be adjusted in the coming years.
- Although changing horizontal and vertical datums will impact all geospatial data a decade from now, such datum changes will not hamper an initial implementation of a National Enhanced Elevation Program, regardless of the elevation data Quality Level selected. When the new geometric reference frame is implemented in the 2020's, new elevation data will be produced to the new datum and existing elevation data can be converted from the current North American Vertical Datum of 1988 (NAVD 88) to the new vertical datum.
- As LiDAR technology continues to mature, changing hardware and software trends will not hamper a consistent implementation of nationwide LiDAR but will provide additional tools for data providers and professional users, and quick/simple 3-D viewing options for non-professional users.
- Future improvements to LiDAR hardware and software could impact the overall Benefit Cost Analysis performed for the NEEA because these improvements are expected to result in lower costs for acquisition and processing of data and new potential benefits; these future improvements would not suggest a delay in implementation because elevation technologies will continue to improve.
- When considering any of the eight program implementation scenarios explained in Section 8, the capacity risk is minimal. USGS' *LiDAR Guidelines and Base Specifications* must be finalized for LiDAR QL1, QL2 and/or QL3 data before initiating a consistent implementation of nationwide LiDAR at any of these Quality Levels. Intermap's "Product Handbook and Quick Start Guide" already *serves as the consistent Guidelines and* Specifications for airborne IFSAR data of the U.S. including DTMs, DSMs and ORIs. Potential revisions to USGS' *LiDAR Guidelines and Base Specifications* should have no significant impact on the overall Benefit Cost Analysis performed for the NEEA unless new requirements are added that increase the pricing per square kilometer.
- For consistent implementation of na*tionwide LiDAR, it is imperative that co*nsistent LiDAR Guidelines and Base Specifications be used and that independent QA/QC be performed in a consistent manner nationwide. Potential changes to QA/QC procedures will have no significant impact on the overall Benefit Cost Analysis performed for the NEEA unless new QA/QC requirements are added that cannot be satisfied by the 15% added costs estimated for survey of QA/QC checkpoints and independent QA/QC.
- For consistent implementation of nationwide LiDAR, the program would need to operate against a clear set of standards for data collection and derivative product generation.
- For either topographic data or bathymetric data, reliable elevation data must be available from USGS, NOAA, FEMA and/or other cooperating partners before anybody (e.g., Google, Microsoft, ESRI, OpenTopography Portal, etc.) can serve it to the public for the hundreds of diverse applications highlighted in this report. Any solution for elevation data needs to include adequate

resources for lifecycle management and maintenance. Conservatively-estimated benefits from federal, state, county, regional, city/town and tribal governments were all significantly understated in the Benefit Cost Analysis. Furthermore, Dewberry determined that it would be premature to count major benefits expected to occur as a result of elevation-based roadway geometry required for Intelligent Transportation System (ITS), IntelliDrive, and/or Advanced Driver Assistance System (ADAS) initiatives that are expected to save lives as well as billions of dollars annually for America's drivers. For these reasons, Dewberry expects that future changes to benefits in the Benefit Cost Analysis will cause most B/C Ratios and net benefits to increase rather than decrease.